



The computational modeling of problems on domains with small holes

Ivo Babuška^a, Ana Maria Soane^{b,*}, Manil Suri^c

^a ICES, 201 East 24th Street, University of Texas at Austin, Austin, TX 78712, United States

^b Department of Mathematics, U.S. Naval Academy, 121 Blake Road, Annapolis, MD 21402, United States

^c Department of Mathematics and Statistics, University of Maryland Baltimore County, 1000 Hilltop Circle, Baltimore, MD 21250, United States

Received 24 May 2016; received in revised form 7 May 2017; accepted 8 May 2017

Available online 15 May 2017

Highlights

- Intuitive limiting model inaccurate, misleading convergence tests.
- Correct model must account for holes with finite radius.
- Modified FEM treats domains with holes without meshing holes.
- Extremely fast FE convergence because unknowns are smooth.
- Method recovers forces on hole boundaries better than asymptotic limit.

Abstract

The modeling challenges arising when the problem domain has small supported holes in it are considered through a representative membrane problem. Such problems are sometimes modeled intuitively in engineering practice by taking the limiting case of holes with zero radius. This intuitive model is incorrect, since it has no mathematical solution. It is demonstrated, however, that finite element approximations based on it can still satisfy verification tests and appear to converge, leading to erroneous recovery of quantities of interest. This points to the need for an alternate approach where the holes of finite radius are properly incorporated in the modeling, and robustness with respect to the radius is maintained. To this end, a computational method is presented which combines analytic knowledge of the solution singularities with finite element approximation of its smooth components. Theoretical and numerical results are provided, establishing the efficacy and robustness of the method in extracting quantities of interest. The method converges both with respect to the size of the holes and the mesh discretization parameter, and provides a more accurate alternative to using the asymptotic limit.

Published by Elsevier B.V.

Keywords: Finite elements; Logarithmic singularities; Prestressed membrane; Perforated domain; Verification; Validation

* Corresponding author.

E-mail addresses: babuska@ices.utexas.edu (I. Babuška), soane@usna.edu (A.M. Soane), suri@umbc.edu (M. Suri).

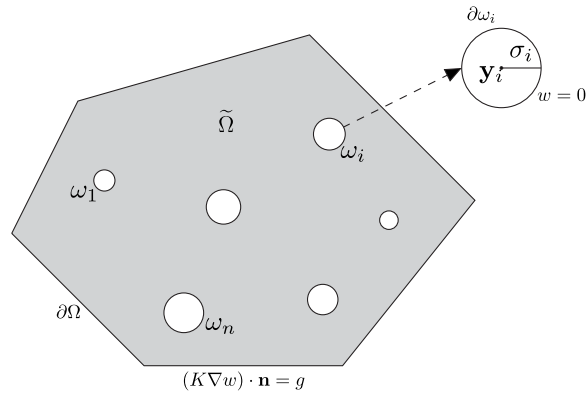


Fig. 1. Sample domain.

1. Introduction

We consider the flat prestressed membrane Ω shown in Fig. 1, attached to supporting discs ω_i , $i = 1, 2, \dots, n$, with distributed normal stress g acting on its boundary $\partial\Omega$ (i.e. the membrane has Dirichlet conditions on $\partial\omega_i$ and Neumann conditions on $\partial\Omega$). Our goal in this paper is to analyze two different approaches to modeling this problem in the case that the radii σ_i of the discs ω_i are *small*. We address both the choice of underlying mathematical model and of the method of discretization. Our results apply to several mathematically equivalent problems such as heat transfer in the presence of cooling pipes, anti-plane elasticity analysis of material reinforced by steel wires or rods, electrostatics problems with wires running through the domain, etc., all of which can be addressed by the same models we consider.

For most problems, a selection or hierarchy of different mathematical models is usually available. The general principle behind which one to choose involves balancing the complexity, accuracy and ease of computational resolution of the model with the reliability of available input data and the nature and accuracy of the output information desired. In particular, any model and its method of discretization should be judged in terms of the goals of the computation, i.e. how accurately these deliver specific user-selected *quantities of interest* (QoI), as opposed to other possible outputs.

Model *validation* refers to estimating the reliability of the underlying mathematical model. In engineering, this may be accomplished by some combination of intuition, experience, qualitative appraisal of the solution (e.g. through graphs and figures or comparison with experimental results), and mathematical analysis. The *verification* component, which refers to the estimation of error due to numerical implementation, may then be performed by simple methods like comparing the results obtained by two discretizations, or by more mathematically sophisticated means, e.g. *a posteriori* error estimation (see e.g. [1–3]).

The first mathematical model we consider, our “Basic Model”, is one of the simplest choices for our flat prestressed membrane (and the other problems mentioned). It is described by the second-order linear PDE

$$-\nabla \cdot (K(\mathbf{x})\nabla w(\mathbf{x})) = 0, \quad \mathbf{x} \in \tilde{\Omega} \quad (1)$$

$$(K(\mathbf{x})\nabla w(\mathbf{x})) \cdot \mathbf{n}(\mathbf{x}) = g(\mathbf{x}), \quad \mathbf{x} \in \partial\Omega \quad (2)$$

$$w(\mathbf{x}) = 0, \quad \mathbf{x} \in \partial\omega, \quad (3)$$

where $\tilde{\Omega}$ represents the domain outside the discs and $\partial\omega$ the combined boundary of the discs. Here, $w(\mathbf{x})$ is the vertical displacement and $\mathbf{n}(\mathbf{x})$ the outward normal to $\tilde{\Omega}$ at the point \mathbf{x} . The positive definite matrix $K(\mathbf{x})$ relates to membrane prestressing and can be replaced by a constant if we know from the fabrication that it does not vary much. This Basic Model will be reasonably accurate when g is assumed small enough for effects to be essentially linear. (Note that we focus on the problem with Neumann boundary conditions on $\partial\Omega$ and Dirichlet boundary conditions on $\partial\omega$.)

Let us define the following two QoI, the determination of which will be the goals of our calculation. First, the energy

$$E(w, S) = \int_S (K \nabla w) \cdot \nabla w \, d\mathbf{x} \quad (4)$$

of the solution in subdomains $S \subset \Omega$ not close to the discs (i.e. $\text{dist}(\partial S, \partial \omega) > \rho > 0$). Second, the forces q_i acting on the boundaries of the discs, defined by

$$q_i(w) = \int_{\partial \omega_i} (K \nabla w) \cdot \mathbf{n} \, ds. \quad (5)$$

In keeping with the principles mentioned earlier, these QoI will form the basis for our evaluation of any model and its method of discretization. For the Basic Model discretized by the standard FEM, both verification and validation are well-established with respect to these (and other) QoI when g is in a suitable range.

Since our concern in this paper is the case when the radii of the discs are small, we can propose an even simpler model, where σ_i are just taken to be 0. This limiting case yields an easier domain to work with, since the onerous task of meshing the discs (which requires human input, and can dominate the cost of modeling) is avoided. For this model, (3) is replaced by the limiting point constraints

$$w(\mathbf{y}_i) = 0, \quad i = 1, 2, \dots, n, \quad (6)$$

where \mathbf{y}_i is the center of disc ω_i . We call (1), (2), (6) the “Intuitive Model”.

Although seemingly natural and intuitively clear, the Intuitive Model is *incorrect*, since the point boundary conditions (6) are inadmissible for second-order PDEs like (1) over domains in two and higher dimensions. Mathematically, the exact solution does not exist, since the energy $E(w, \tilde{\Omega})$ and $L_2(\tilde{\Omega})$ norm of w increase without bound as $\sigma_i \rightarrow 0$, becoming infinite in the limit.

And yet, a finite element discretization of the Intuitive Model can always be carried out, since (6) just reduces to a set of point constraints $w_h(\mathbf{y}_i) = 0$ on the finite element solution w_h . Although the energy of w_h will become infinite as $h \rightarrow 0$, it remains finite for any $h > 0$, so that w_h always exists and is unique. The question then arises whether these FE approximations for the “incorrect” limiting case $\sigma_i = 0$ can be used to produce reasonable-looking approximations for the QoI for the case $\sigma_i \geq 0$.

The answer is yes. Even though $E(w_h, \tilde{\Omega})$ and $\|w_h\|_{L_2(\tilde{\Omega})}$ diverge as $h \rightarrow 0$, we can, indeed, extract values for our two QoI from w_h that pass verification tests such as “converging” numerically, i.e. yielding acceptable error estimates based on the comparison for two step sizes h and $h/2$ (see Section 8). This is one of the key motivations behind our paper – the fact that certain quantities of interest may still be recovered even when the model is incorrect and an exact solution does not exist – a situation that can occur often enough in actual engineering and scientific practice. For example, such a case of ill-posed point constraints being used to analyze the elastostatics of the Faraday cage by Feynman in his classic work [4] was recently pointed out in [5,6]. As another example, engineering computations in elasticity (a natural extension of the problem considered here) often use strategies where connections between domain components (say by rivets passing through holes, see e.g. [7]) are implemented by matching nodal displacements, a constraint which can be just as inadmissible as a point boundary condition. A third specific example is the lug problem in Section 17.1 of [8] (results from which are commented on in Section 8).

The crucial issue that arises then is how reliable are these approximations? We address this by investigating two related questions. First, do the QoI corresponding to the Basic Model have well-defined limits as $\sigma_i \rightarrow 0$? We show in Sections 4 and 5 that even though the solution w of the Basic Model does not converge in the energy norm, there exists $u_0 \in L_2(\Omega)$ such that the QoI $E(w, S)$ converges to $E(u_0, S)$ (Theorem 5.4). Moreover, the QoI $q_i(w)$ also has a well-defined limit q_i^0 as $\sigma_i \rightarrow 0$, which can be analytically computed (Theorem 5.6). However, our theorems show that the convergence of our QoI to their asymptotic limits is only logarithmic. So the asymptotic $\sigma_i = 0$ values may not be practically acceptable approximations to the QoI actually needed (where $\sigma_i > 0$) unless the discs are extremely small. We demonstrate this computationally in Section 7, where holes of unequal radii are seen to cause unacceptably large deviations in the QoI from their asymptotic limits.

The second question, investigated in Section 8, is how well values recovered from the FE approximations of the Intuitive Model approximate our QoI. We show that the fact that successive step sizes give very close results can be a misleading test, particularly when the “converged” computed values are used to approximate QoI for $\sigma_i > 0$. While the intuitive FE approximations may converge to the limiting values $E(u_0, S)$ and q_i^0 , the observed convergence

rate can be slow, and as pointed out in [8], other limits might be possible, depending on the meshes used. Hence, a clear understanding of the asymptotic values of the QoI is needed before any conclusions can be drawn. Our recommendation therefore is to use the Basic Model, not the Intuitive Model.

The need for the Basic Model then brings us to the second key issue we address in this paper: how to efficiently discretize it? As mentioned earlier, modeling the discs can involve meshing costs and moreover, the use of curvilinear elements. Also, the exact solution will contain a component in the vicinity of each disc which gets increasingly singular as $\sigma_i \rightarrow 0$. This may lead to poor approximation by the trial functions, unless highly non-quasiuniform meshes are used (which may again require enhanced human input and lead to a system of FEM equations with very high scaled conditioning number).

We therefore present a modified FEM which incorporates *a priori* analytic knowledge of the singular behavior near discs into the solution procedure. In particular, these singular components are (essentially) reproduced exactly in the approximate solution. This allows us to perform the finite element modeling on a “filled in” domain without discs (which was the fundamental motivation behind the Intuitive Model), thus obviating the need to use curvilinear elements or implement any special meshing. Our method is *robust* with respect to the size of the discs, which can be varied very easily, as required in parameter sensitivity studies. Moreover, the functions being approximated by finite elements are smooth, resulting in high convergence rates for our QoI. Our modified FEM can be easily extended to supports (or holes) of arbitrary shapes (Remark 3.1) and materials with various anisotropies (Remark 3.2). The method is not required for boundary conditions other than the Dirichlet inside/Neumann outside pairing considered here (see Remark 2.2).

An outline of our paper is as follows. In Section 2, we reformulate our model problem into one whose asymptotic limit remains square-integrable as the disc radii $\sigma_i \rightarrow 0$. (This introduces an additional boundary unknown that becomes infinite as $\sigma_i \rightarrow 0$.) In Section 3, we introduce a linear combination of singular and smooth components which serves as an approximate decomposition of the exact solution. The coefficients of this linear combination can be obtained as the solution of a system of equations whose solvability and asymptotics we analyze in Section 4. In Section 5, we derive energy norm estimates for the error between the exact solution and our linear combination as $\sigma_i \rightarrow 0$, and also prove an estimate establishing the effectiveness of our recovery of the QoI q_i (again as $\sigma_i \rightarrow 0$). Section 6 contains error estimates for our modified finite element approximation of the Basic Model, which establish asymptotic convergence rates for our QoI both in terms of $\sigma_i \rightarrow 0$ and $h \rightarrow 0$ (or $p \rightarrow \infty$ in the p version). In Section 7, we report the results of computational experiments, which demonstrate the effectiveness of the modified FEM for a range of parameter values $\sigma_i > 0$ and $h > 0$ of practical interest. Section 8 contains the results of computations to assess how well our QoI is recovered using the Intuitive Model. Finally, in Section 9, we summarize our method and present our conclusions.

Let us mention that the analytic study of problems over domains with small holes (the generalization of our disc exclusions) has a rich history. See, for instance, the works by Il'in (e.g. [9,10]), Maz'ya and collaborators (e.g. [11,12]), Lanza de Cristoforis (e.g. [13,14]), Dalla Riva and collaborators (e.g. [15,16]) and others (e.g. [17–21]). Such studies have also led to computational techniques for the Basic Model that incorporate knowledge of the singularities and use series expansions to approximate the smooth components (see e.g. the meso-scale method in [12] and the least-squares boundary-matching method in [6]). Resolving the smooth components by finite elements, as we propose and analyze in depth in this paper, sets the problem in a natural, convenient and flexible engineering framework, that allows efficient and easily verifiable recovery of QoI and the application of various estimation and postprocessing techniques available in the context of FEM architecture.

In this regard, the idea of incorporating analytic features of the solution in the finite element solution also has many precedents. For instance, enhancing subspaces with corner singularities was discussed early on in [22,23]. More recent developments along these lines include the Generalized Finite Element Method [24,25], the Partition of Unity Method [26] as well as their combination [27]. For some comments on the differences between our method and these approaches see Remark 3.3.

Finally, we are particularly motivated by problems from plane elasticity, such as the design and analysis of lugs and perforated connectors (see Remarks 2.3 and 2.4). Our method can be extended to such elasticity problems, as well as to other operators including the 3D Laplacian (see Remarks 3.2 and 4.3).

2. Mathematical formulation of the basic model

Let $\Omega \subset \mathbb{R}^2$ be a domain with piecewise smooth boundary $\partial\Omega$ as shown in Fig. 1. The discs ω_i , $i = 1, 2, \dots, n$ (or “holes” as we will refer to them in the sequel) will be assumed to satisfy $\bar{\omega}_i \subset \Omega$, and $\bar{\omega}_i \cap \bar{\omega}_j = \emptyset$, $i \neq j$. Denote

$\omega = \cup_{i=1}^n \omega_i$, $\partial\omega = \cup_{i=1}^n \partial\omega_i$, and $\tilde{\Omega} = \Omega \setminus \bar{\omega}$. Let $g \in L_2(\partial\Omega)$. Taking $K = 1$ for simplicity, we may write (1), (2), (3) as the Laplace equation problem,

$$-\Delta w = 0 \text{ in } \tilde{\Omega} \tag{7}$$

$$\frac{\partial w}{\partial n} = g \text{ on } \partial\Omega \tag{8}$$

$$w = 0 \text{ on } \partial\omega. \tag{9}$$

Define $H_D^1(\tilde{\Omega}) = \{w | w \in H^1(\tilde{\Omega}), w = 0 \text{ on } \partial\omega\}$. Then there is unique $w \in H_D^1(\tilde{\Omega})$ such that

$$B_{\tilde{\Omega}}(w, v) = \int_{\tilde{\Omega}} \nabla w \cdot \nabla v \, d\mathbf{x} = F(v) = \int_{\partial\Omega} g v \, ds, \tag{10}$$

for all $v \in H_D^1(\tilde{\Omega})$. The bilinear form $B_{\tilde{\Omega}}$ gives rise to the following energy norm,

$$\|w\|_{E, \tilde{\Omega}} = (B_{\tilde{\Omega}}(w, w))^{\frac{1}{2}}$$

which is equivalent to the $H^1(\tilde{\Omega})$ norm for functions in $H_D^1(\tilde{\Omega})$ as long as the radii $\sigma_i > 0$. We define the corresponding energy space as $\mathcal{E}(\tilde{\Omega})$, where for any $S \subset \tilde{\Omega}$,

$$\mathcal{E}(S) = \{w | E(w, S) = B_S(w, w) = \|w\|_{E,S}^2 < \infty\}.$$

Let us define

$$G = \int_{\partial\Omega} g(\mathbf{x}) \, ds. \tag{11}$$

Then we see by (7) that

$$\int_{\partial\omega} \frac{\partial w}{\partial n} \, ds = -G,$$

which means that defining

$$q_i = \int_{\partial\omega_i} \frac{\partial w}{\partial n} \, ds \tag{12}$$

(as in (5)), we must have

$$\sum_{i=1}^n q_i = -G. \tag{13}$$

This shows that the total force G gets distributed over the boundaries of the separate internal holes. Consequently, as the holes become smaller (i.e. $\sigma_i \rightarrow 0$) we can expect, in an average sense,

$$\frac{\partial w}{\partial n} \approx \frac{q_i}{|\partial\omega_i|} = q_i(2\pi\sigma_i)^{-1} \text{ on } \partial\omega_i.$$

This shows that $\frac{\partial w}{\partial n}$ will become unbounded at $\partial\omega$ as $\sigma_i \rightarrow 0$. In fact, the solution cannot lie in $H^1(\Omega)$ in the limit, since (9) would then reduce to a point constraint, which would be inadmissible. As it turns out, we can expect the solution to get unbounded *everywhere* outside $\partial\omega$ as $\sigma_i \rightarrow 0$, as may be seen from the simple case of an annulus.

Example 2.1. Suppose Ω is the unit circle, and there is only one hole, ω , which is a circle of radius σ with center at the origin. For simplicity, suppose $g = 1$ on $\partial\Omega$. Then it may be easily verified that the solution to (7)–(9) is given by

$$w(r, \theta) = \log r - \log \sigma \tag{14}$$

where (r, θ) are polar coordinates at the origin. From this, we may observe that $\int_{\tilde{\Omega}} w \, d\mathbf{x} = O(|\log \sigma|)$, $\|w\|_{0, \tilde{\Omega}} = O(|\log \sigma|)$, $|w|_{1, \tilde{\Omega}} = O(|\log \sigma|^{\frac{1}{2}})$, and $\|w\|_{2, \tilde{\Omega}} = O(\sigma^{-1})$.

Remark 2.1. The case of a general Ω with multiple holes can also be expected to exhibit unboundedness in similar norms. In this general case, the energy norm is given by

$$\|w\|_{E, \tilde{\Omega}}^2 = |w|_{1, \tilde{\Omega}}^2 = \int_{\tilde{\Omega}} \nabla w \cdot \nabla w \, d\mathbf{x} = \int_{\partial\Omega} g w \, ds.$$

Since we expect this to be unbounded as $\sigma_i \rightarrow 0$, we see that w cannot remain bounded on $\partial\Omega$. This essentially implies that w will have a (constant) component similar to $\log \sigma$ in (14) that makes it unbounded everywhere as $\sigma_i \rightarrow 0$.

Remark 2.2. We analyze the case of Dirichlet conditions on $\partial\omega_i$ and Neumann conditions on $\partial\Omega$ precisely because of the above singularities and unbounded behavior. If Dirichlet conditions are imposed on $\partial\Omega$, then the problem remains well-posed in the limit $\sigma_i \rightarrow 0$. Also, the problem with Neumann conditions on all boundaries will have a solution (and be well-posed) if and only if a compatibility condition is satisfied by the boundary data. Hence the special method we develop in this paper is not needed for any of these cases.

Remark 2.3. As mentioned in the introduction, our model problem has many applications and extensions. One is the lug problem in elasticity discussed in [8] and others, where Ω is the lug and ω_i the fasteners. Instead of (7), we have a system of equations in the displacement $u = (u_x, u_y)$. Also, our QoI q_i is a three-dimensional vector representing the forces in the x and y directions and the moment over the fastener boundaries, the determination of which is of particular engineering significance.

From (14) and Remark 2.3, we note that the unboundedness of w in the L_2 norm as $\sigma \rightarrow 0$ is due to the constant $\log \sigma$ term (as opposed to the $\log r$ term, which remains bounded in L_2). Let us therefore reformulate (7)–(9) by essentially removing the constraint (9), which is the cause of this $\log \sigma$ term appearing. (This will also be necessary for solving a linear system of equations we encounter in Section 4.) We now find a u satisfying (Fig. 2):

$$-\Delta u = 0 \text{ in } \tilde{\Omega} \quad (15)$$

$$\frac{\partial u}{\partial n} = g \text{ on } \partial\Omega \quad (16)$$

$$u = A \text{ on } \partial\omega \quad (17)$$

$$\int_{\tilde{\Omega}} u(\mathbf{x}) \, d\mathbf{x} = 0. \quad (18)$$

Here, A is an unknown real number, and this extra degree of freedom is compensated for by the additional constraint (18), so that we once again have existence and uniqueness. In fact, the solutions u and w simply differ by a constant. Indeed, define $A^* = \int_{\tilde{\Omega}} w(\mathbf{x}) \, d\mathbf{x}$. Then $u = w - A^*/|\tilde{\Omega}|$ satisfies (15)–(18) with $A = -A^*/|\tilde{\Omega}|$.

Since we expect A^* to be unbounded as $\sigma_i \rightarrow 0$, A will be as well, i.e. the value of u will now be allowed to blow up at the holes (instead of being constrained to 0). However, as we will see, the L_2 norm of u will now remain bounded — this is the analog of saying that if we remove the $\log \sigma$ term in (14), then the $\log r$ term that remains will be L_2 bounded. Note that since $\|w\|_{E, \tilde{\Omega}} = \|u\|_{E, \tilde{\Omega}}$, the unboundedness in the energy norm will be unaffected.

Remark 2.4. The physical interpretation of the reformulation is that the membrane is supported by discs attached to a rigid board which (instead of being fixed at zero height) can move vertically up or down an amount A . In the lug problem, the board would be able to move in the x and y directions and also rotate.

Remark 2.5. Since the value of A is an unknown, the solution to (15)–(18) is the pair (u, A) . Note that our QoI for this reformulation are the same as for (7)–(9), independently of A and (18).

Since we are interested in the case of small holes, let us use a parameter $\kappa \in (0, 1]$ to formalize the way their radii can tend to 0. We assume that $\rho_i, i = 1, 2, \dots, n$ are fixed values satisfying $0 < \rho_i \leq R < 1$. Here, R will be assumed to be small enough — a sufficient condition will be given in Section 4. Define

$$\sigma_i(\kappa) = \kappa \rho_i. \quad (19)$$

The holes will now be the circular domains $\omega_i(\kappa)$ with centers \mathbf{y}_i and radii $\sigma_i(\kappa)$. Define $\omega(\kappa) = \cup_{i=1}^n \omega_i(\kappa)$ and let $\tilde{\Omega}(\kappa) = \Omega - \bar{\omega}(\kappa)$. Then we denote by $(u(\kappa), A(\kappa))$ (respectively $w(\kappa)$) the solution of (15)–(18) (respectively (7)–(9)) on $\tilde{\Omega}(\kappa)$.

Let us denote $\mathcal{S} = \{S \subset \Omega \mid \text{dist}(S, \cup_{i=1}^n \mathbf{y}_i) > 0\}$. Although $\|u(\kappa)\|_{E, \tilde{\Omega}}$ does not converge as $\kappa \rightarrow 0$, in Section 5 (see Theorem 5.4), we will show that there exists unique $u_0 \in L_2(\Omega)$ such that $\forall S \in \mathcal{S}, u_0 \in \mathcal{E}(S)$ and $\|u(\kappa) - u_0\|_{E, S} \rightarrow 0$ as $\kappa \rightarrow 0$. (Here, for any S, κ is assumed small enough so that $S \subset \tilde{\Omega}(\kappa)$.)

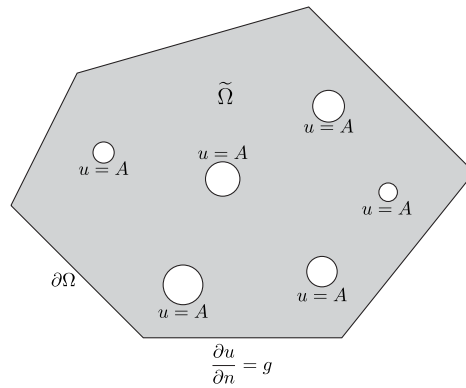


Fig. 2. Solution u .

3. An approximation to the solution

In this section, we construct $U(\kappa)$, a linear combination of singular and smooth components, which will approximate $u(\kappa)$ in $\|\cdot\|_{E, \tilde{\Omega}}$ (i.e. in the $H^1(\tilde{\Omega})$ seminorm). Further approximating the smooth components by the finite element method (as indicated in Section 6) will lead to our computational solution.

We will need $G \neq 0$ in our algorithm, which we assume from now on. In case $G = 0$ or G is small, we can instead solve two problems, taking $g_1 = g + 1$ and $g_2 = 1$ in the boundary condition (8), and obtaining our solution as the difference.

For the singular components, we will be guided by the annulus example, which indicates that $u(\kappa)$ can be expected to grow logarithmically near the holes. Hence we take these components to be

$$\phi_i(\mathbf{x}) = \log|\mathbf{x} - \mathbf{y}_i|. \tag{20}$$

Note that

$$-\Delta\phi_i = 2\pi\delta_i \text{ in } \Omega, \tag{21}$$

where δ_i is the Dirac function at \mathbf{y}_i . Hence ϕ_i is harmonic on $\Omega - \mathbf{y}_i$.

These components ϕ_i will result in stresses $\partial\phi_i/\partial n$ on $\partial\Omega$ which satisfy

$$\int_{\partial\Omega} \frac{\partial\phi_i}{\partial n} ds = 2\pi. \tag{22}$$

Our smooth components ψ_i will be defined to correct for these boundary stresses, with the aim of enforcing (16). For this, we let $\psi_i \in H^1(\Omega)$ satisfy

$$-\Delta\psi_i = 0 \text{ in } \Omega \tag{23}$$

$$\frac{\partial\psi_i}{\partial n} = \frac{2\pi}{G}g - \frac{\partial\phi_i}{\partial n} \text{ on } \partial\Omega. \tag{24}$$

Noting that

$$\begin{aligned} \int_{\partial\Omega} \frac{\partial\psi_i}{\partial n} ds &= \int_{\partial\Omega} \left(\frac{2\pi}{G}g - \frac{\partial\phi_i}{\partial n} \right) ds \\ &= 2\pi \int_{\partial\Omega} \frac{g}{G} ds - \int_{\partial\Omega} \frac{\partial\phi_i}{\partial n} ds = 2\pi(1) - 2\pi = 0, \end{aligned}$$

we see that (23)–(24) has a solution that is unique up to a constant. To specify this constant, we can impose the additional requirement,

$$\int_{\Omega} \psi_i(\mathbf{x}) d\mathbf{x} = 0. \tag{25}$$

However, specifying a different constant (via some other condition) does not change our approximation to $w(\kappa)$, see [Theorem 4.4](#). This flexibility can come into play while trying to define $U(\kappa)$, see [Remark 4.4](#).

Unlike ϕ_i , we do not know the functions ψ_i explicitly, so we will approximate them by the finite element method. Note that ψ_i are defined on the entire domain Ω , so such approximation can be carried out without modeling the holes. Moreover, each ψ_i is a smooth function (with smoothness determined only by the regularity of the domain Ω) since the forcing terms in (24) are smooth and independent of κ . This is an essential feature of our approach: separating out the singular functions ϕ_i so that the smooth ψ_i can be well approximated by finite elements of any order on a uniform mesh.

We now define $U(\kappa) \in H^1(\tilde{\Omega}(\kappa))$ to be the linear combination,

$$U(\kappa) = \sum_{i=1}^n c_i(\kappa)(\phi_i + \psi_i), \quad (26)$$

where $\mathbf{c}(\kappa) = (c_1(\kappa), c_2(\kappa), \dots, c_n(\kappa))^T \in \mathbb{R}^n$ is to be determined. Then clearly $U(\kappa)$ is harmonic on $\tilde{\Omega}(\kappa)$. Physically speaking, c_i is approximately $-1/2\pi$ times the force q_i acting on the boundary of the disc ω_i (see Eq. (66) ahead). With this in mind, the first condition we impose to specify $\mathbf{c}(\kappa)$ is essentially (13), i.e.

$$\sum_{i=1}^n c_i(\kappa) = \frac{G}{2\pi}. \quad (27)$$

Then, using (24), (26) and (27),

$$\frac{\partial U(\kappa)}{\partial n} = \sum_{i=1}^n c_i(\kappa) \left(\frac{2\pi}{G} g \right) = g \text{ on } \partial\Omega,$$

so that $U(\kappa)$ satisfies the same boundary condition (16) as $u(\kappa)$.

Next, for $U(\kappa)$ to be a good approximation to $u(\kappa)$, we should also have it assume a common constant value along all of the boundaries $\partial\omega_i(\kappa)$ (in the same way that $u(\kappa)$ reduces to $A(\kappa)$ in Eq. (17)). We satisfy this condition only in an average sense, by introducing a new unknown $d(\kappa) \in \mathbb{R}$ (corresponding to $A(\kappa)$), and imposing the n equations

$$\frac{1}{\text{meas}(\partial\omega_i)} \int_{\partial\omega_i} U(\kappa)(s) ds = d(\kappa), \quad i = 1, 2, \dots, n. \quad (28)$$

(Noting that κ is small, we see this does give $U(\kappa) \approx d(\kappa)$ on $\partial\omega_i$.)

Since ψ_j is harmonic on ω_i for $i, j = 1, 2, \dots, n$, we have the identities,

$$\psi_j(\mathbf{y}_i) = \frac{1}{2\pi\sigma_i} \int_{\partial\omega_i} \psi_j(s) ds, \quad (29)$$

with an analogous relation holding for ϕ_j over $\partial\omega_i$, $j \neq i$. Substituting (26) in (28) and using these identities, we get the n equations

$$c_i(\kappa) \log \sigma_i(\kappa) + \sum_{j=1, j \neq i}^n c_j(\kappa) \phi_j(\mathbf{y}_i) + \sum_{j=1}^n c_j(\kappa) \psi_j(\mathbf{y}_i) = d(\kappa), \quad i = 1, 2, \dots, n. \quad (30)$$

Then (27), (30) is a system of $n + 1$ linear equations in the $n + 1$ unknowns $(\mathbf{c}(\kappa), d(\kappa))$. (This balancing of constraints and unknowns is another reason we transformed our original problem in $w(\kappa)$ to one in $u(\kappa)$, which had the extra unknown $A(\kappa)$.)

Remark 3.1. Our method extends easily to holes of other shapes by using Eq. (28) to recalculate the coefficients of c_j , $j = 1, 2, \dots, n$ in Eq. (30). For an ellipse or square, for instance, only the coefficient $\log \sigma_i(\kappa)$ changes, but for more general shapes where an analog of (29) does not hold, $\phi_j(\mathbf{y}_i)$, $\psi_j(\mathbf{y}_i)$ must also be replaced by averages of ϕ_j , ψ_j , respectively, over $\partial\omega_i$.

Remark 3.2. Observe that the singular component (20) corresponds to the fundamental solution for the problem, i.e. the solution for the case of a concentrated load at the point \mathbf{y}_i (Eq. (21)). Our idea can therefore be applied to other operators as well, by taking ϕ_i to be the corresponding fundamental solution. For instance, we have taken

$K = 1$ in Eq. (1) for simplicity, but various anisotropies with general K could be treated, using the corresponding fundamental solutions (available in references like [28]). Also, the method can readily be extended to elasticity where (in 2D) we will have three singular components for each i , corresponding to concentrated loads in the x and y directions, and to a concentrated moment.

Remark 3.3. The idea of using analytic functions in conjunction with numerical treatment is very natural. As mentioned in the introduction, it was already used in works like [22] in the context of FE approximation of corner singularities. Such enrichments have also been applied locally using partition of unity functions, as in the GFEM and EXFEM (see e.g. [25,27]). Logarithmic singularities have been combined with asymptotic expansions in e.g. [12] and [6].

Let us comment that while partition of unity and GFEM methods use a localized approach to treat various features of the solution, our approach, being global, is both theoretically and implementationally different. In particular, no singularities or handbook solutions need to be locally inserted via specialized basis functions (as, for example, has been done to treat voids by the GFEM in [29]). The advantage of our approach is that it is provably robust with respect to the hole radii, as we establish in this paper. We remark that when our approach is used to treat the holes, partition of unity/enrichment methods could also be incorporated into the approximation procedure to treat other solution features of the types discussed e.g. in [26].

4. The linear equations

In this section, we will show that the linear system (27), (30) has a unique solution. Moreover, we will investigate its solution as $\kappa \rightarrow 0$. For vectors \mathbf{a} , we will use the usual norm $\|\mathbf{a}\| = \max_{1 \leq i \leq n} |a_i|$, and for $n \times n$ matrices A , the norm $\|A\| = \max_{1 \leq i \leq n} \sum_{j=1}^n |A_{ij}|$.

Define \mathbf{e} to be the vector $(1, 1, \dots, 1)^T \in \mathbb{R}^n$. Then we may write Eqs. (30) as

$$M\mathbf{c} = d\mathbf{e} \tag{31}$$

where $M = M(\kappa)$ is an $n \times n$ matrix that has the form

$$M(\kappa) = D(\kappa) + B.$$

Here, $D = \text{diag}\{D_{11}, D_{22}, \dots, D_{nn}\}$ is the diagonal matrix with entries

$$D_{ii} = D_{ii}(\kappa) = \log \sigma_i(\kappa) = \log \rho_i + \log \kappa$$

and $B = \{B_{ij}\}$ is the matrix given by

$$\begin{aligned} B_{ij} &= \psi_j(\mathbf{y}_i) + \phi_j(\mathbf{y}_i), \quad i \neq j \\ &= \psi_i(\mathbf{y}_i), \quad i = j. \end{aligned} \tag{32}$$

Note that B is independent of κ , and by (20)–(25), depends entirely on g , the domain, and the holes. Hence, its norm can be bounded independently of κ . Moreover, since $\sigma_i(\kappa) \leq R < 1$ for any $\kappa \in (0, 1]$, the diagonal entries of D are strictly negative, so that D is invertible.

Define the vector

$$\mathbf{g} = \mathbf{g}(\kappa) = D^{-1}(\kappa) \mathbf{e}.$$

Then we see that

$$\mathbf{g}_i(\kappa) = D_{ii}^{-1}(\kappa) = (\log \sigma_i(\kappa))^{-1} = (\log \rho_i + \log \kappa)^{-1}, \tag{33}$$

so that

$$\|D^{-1}(\kappa)\| = \|\mathbf{g}(\kappa)\| \leq \min\{|\log R|^{-1}, |\log \kappa|^{-1}\}. \tag{34}$$

The matrix M will be diagonally dominant (and hence invertible) provided the holes are small enough. More precisely, the condition (35) in the following lemma is sufficient.

Lemma 4.1. Let R be small enough so that

$$\alpha = \frac{\|B\|}{|\log R|} < \frac{1}{2} \quad (35)$$

where B is as in (32). Then for all $\kappa \in (0, 1]$, the matrix $M(\kappa)$ defined in (31) is invertible, and its inverse satisfies the uniform estimate

$$\|M^{-1}(\kappa)\| \leq 2 \min\{|\log R|^{-1}, |\log \kappa|^{-1}\}. \quad (36)$$

Moreover,

$$M^{-1}(\kappa) = D^{-1}(\kappa)(I + Z(\kappa)) \quad (37)$$

where for all $\kappa \in (0, 1]$,

$$\|Z(\kappa)\| \leq 2\alpha \min\{1, |\log R| |\log \kappa|^{-1}\}. \quad (38)$$

Proof. Let us write

$$M = D + B = (I + BD^{-1})D.$$

Then using (34) and (35), we have

$$\|BD^{-1}\| \leq \|B\| \|D^{-1}\| \leq \alpha \min\{1, |\log R| |\log \kappa|^{-1}\} < \frac{1}{2}.$$

Hence, $I + BD^{-1}$ is invertible, with its inverse given by the convergent infinite series

$$\begin{aligned} (I + BD^{-1})^{-1} &= I - BD^{-1} + (BD^{-1})^2 - (BD^{-1})^3 \dots \\ &= I + Z. \end{aligned} \quad (39)$$

From this, it easily follows that

$$\begin{aligned} \|(I + BD^{-1})^{-1}\| &\leq \frac{1}{1 - \|BD^{-1}\|} < 2, \\ \|Z\| &\leq \frac{\|BD^{-1}\|}{1 - \|BD^{-1}\|} \leq 2\alpha \min\{1, |\log R| |\log \kappa|^{-1}\}, \end{aligned} \quad (40)$$

proving (38). We also see

$$\|M^{-1}\| = \|D^{-1}(I + BD^{-1})^{-1}\| \leq 2\|D^{-1}\|.$$

Estimate (36) follows from (34). \square

Let us define

$$K = |\mathbf{e}^T D^{-1} \mathbf{e}|.$$

Then we have the following lemma.

Lemma 4.2. Let R satisfy (35). Then there exists a constant C independent of κ such that

$$K \geq Cn \min\{|\log \rho_i|^{-1}, |\log \kappa|^{-1}\}. \quad (41)$$

$$|\mathbf{e}^T M^{-1} \mathbf{e}| \geq K(1 - 2\alpha) > 0. \quad (42)$$

Proof. We see that since the terms D_{ii}^{-1} are all negative,

$$K = \left| \sum_i^n D_{ii}^{-1} \right| = \sum_i^n |(\log \sigma_i)^{-1}| \geq n \min_i |(\log \sigma_i)^{-1}|,$$

from which (41) follows. Moreover, since D^{-1} is symmetric,

$$|\mathbf{e}^T D^{-1} \mathbf{Z} \mathbf{e}| = |(D^{-1} \mathbf{e})^T \mathbf{Z} \mathbf{e}| \leq K \|Z\| \leq K(2\alpha), \quad (43)$$

using (38). By (37),

$$|\mathbf{e}^T M^{-1} \mathbf{e}| \geq |\mathbf{e}^T D^{-1} \mathbf{e}| - |\mathbf{e}^T D^{-1} \mathbf{Z} \mathbf{e}|.$$

The estimate (42) follows from (43). \square

Lemma 4.3. *Let R satisfy (35). Then*

$$\|(\log \kappa) M^{-1}(\kappa) - I\| = O(|\log \kappa|^{-1})$$

as $\kappa \rightarrow 0$.

Proof. Factoring $(\log \kappa)^{-1}$ from (33), we note that

$$\|(\log \kappa) D^{-1}(\kappa) - I\| = O(|\log \kappa|^{-1})$$

as $\kappa \rightarrow 0$. Moreover, using (40), we see that $\|Z(\kappa)\| = O(|\log \kappa|^{-1})$ as $\kappa \rightarrow 0$. The lemma follows from (37). \square

Theorem 4.4. *Let R satisfy (35). Then for any $\kappa \in (0, 1]$, the system (27), (30) has a unique solution $(\mathbf{c}(\kappa), d(\kappa))$ satisfying*

$$\|\mathbf{c}(\kappa)\| \leq C|G| \tag{44}$$

with C a constant independent of κ . Moreover, as $\kappa \rightarrow 0$,

$$\|\mathbf{c}(\kappa) - \mathbf{c}(0)\| = O(|\log \kappa|^{-1}) \tag{45}$$

with the limiting solution $\mathbf{c}(0)$ given by

$$c_i(0) = \frac{G}{2\pi n}. \tag{46}$$

Finally, if the functions ψ_i in (26) are replaced by $\psi_i + k_i$ where k_i are arbitrary constants, then the unique solution of the updated system (27), (30) is $(\mathbf{c}(\kappa), d(\kappa) - \sum_{i=1}^n k_i c_i(\kappa))$.

Proof. Since M is invertible, we can solve Eq. (31) for \mathbf{c} to obtain

$$\mathbf{c} = dM^{-1}\mathbf{e}. \tag{47}$$

Substituting in (27),

$$\mathbf{e}^T \mathbf{c} = d\mathbf{e}^T M^{-1} \mathbf{e} = \frac{G}{2\pi}. \tag{48}$$

Since by (42), $\mathbf{e}^T M^{-1} \mathbf{e} \neq 0$, we can solve (48) (and substitute in (47)) to get the unique solution

$$d = \frac{1}{\mathbf{e}^T M^{-1} \mathbf{e}} \frac{G}{2\pi} \tag{49}$$

$$\mathbf{c} = \frac{M^{-1} \mathbf{e}}{\mathbf{e}^T M^{-1} \mathbf{e}} \frac{G}{2\pi}. \tag{50}$$

Next, noting that $\|M^{-1} \mathbf{e}\| = \|M^{-1}\|$, we see, using (36) and (42) that

$$\begin{aligned} \|\mathbf{c}\| &= (2\pi)^{-1} \frac{\|M^{-1}\|}{|\mathbf{e}^T M^{-1} \mathbf{e}|} |G| \\ &\leq C \frac{|\log \kappa|^{-1}}{K} |G|, \end{aligned}$$

so that (44) follows by (41). Eq. (46) follows by taking the limit in (50) and using Lemma 4.3.

Finally, replacing function ψ_i in (26) by $\psi_i + k_i$ has the effect of changing Eq. (31) to

$$(M + [k_1 \mathbf{e} \ k_2 \mathbf{e} \ \dots \ k_n \mathbf{e}])\mathbf{c} = d\mathbf{e},$$

which is equivalent to

$$M\mathbf{c} = \left(d - \sum_{i=1}^n k_i c_i \right) \mathbf{e} = \tilde{d}\mathbf{e}.$$

Hence the new solution is (\mathbf{c}, \tilde{d}) . \square

Remark 4.1. Using (49) and Lemma 4.3, we see that

$$\frac{d}{\log \kappa} \rightarrow \frac{G}{2\pi n}.$$

This shows that $|d|$ is not bounded as $\kappa \rightarrow 0$, but grows as $O(|\log \kappa|)$.

Remark 4.2. We have analyzed the case (19), where the radii of the holes are all proportional to κ . But if we assume they shrink at different rates, the limiting solution may be different. For instance, under the condition

$$\sigma_i(\kappa) = \kappa^{\gamma_i} \rho_i,$$

it is easy to see that Lemma 4.3 holds with I replaced by $J = \text{diag}\{\gamma_1, \gamma_2, \dots, \gamma_n\}$. In this case, the limiting solution $\mathbf{c}(0)$ will be given by

$$c_i(0) = \frac{\gamma_i}{\gamma} \left(\frac{G}{2\pi} \right) \quad (51)$$

where $\gamma = \sum \gamma_i$.

Remark 4.3. We have taken ϕ_i to be logarithmic functions, which come from solving Laplace's equation in two dimensions. As mentioned in Remark 3.2, we can extend our method to other operators by taking ϕ_i to be the corresponding fundamental solutions. The results above will again hold, since these ϕ_i will again be unbounded at $r = 0$. The key property of diagonal dominance of the matrix M when the holes are small enough remains the same, though the exact form of Lemma 4.3 and the limiting solution $c_i(0)$ may change.

As an example, consider the case of Laplace's equation in three dimensions, where the holes are now spheres of radii $\kappa\rho_i$ and the singular components originating at sphere centers \mathbf{y}_i are

$$\phi_i(\mathbf{x}) = \frac{1}{|\mathbf{x} - \mathbf{y}_i|}.$$

Then with $J = \text{diag}\{\rho_1, \rho_2, \dots, \rho_n\}$, and R small enough, we may show (compare with Lemma 4.3)

$$\|\kappa^{-1} M^{-1}(\kappa) - I\| = O(\kappa)$$

as $\kappa \rightarrow 0$. This leads to the limiting solution

$$c_i(0) = \frac{\rho_i}{\rho} \left(\frac{G}{2\pi} \right)$$

where $\rho = \sum \rho_i$. The 2D elasticity problem will also in general lead to coefficients that are different for different i .

Remark 4.4. The condition (35) imposed on R in Theorem 4.4 only guarantees solvability when the holes are small enough. Indeed, when (35) is not satisfied, one may encounter isolated values of κ for which the matrix $M(\kappa)$ is not invertible. Suppose $\text{rank } M = n - 1$, then some column C_i of M would be a linear combination of the other columns C_j , $j \neq i$.

Recall that Eqs. (23)–(24) only define ψ_i up to an arbitrary constant. So in this situation, we can replace ψ_i by $\psi_i + 1$ in the definition of $U(\kappa)$. This has the effect of adding the vector \mathbf{e} to column C_i of M . Then, except for the extremely rare coincidence of \mathbf{e} also happening to be a linear combination of the columns C_j , $j \neq i$, this updated M will now be nonsingular. (If the singular M had rank deficiency $k > 1$, then we could redefine k of the ψ_i 's this way.)

As proved in Theorem 4.4, such replacement does not change the solved coefficients \mathbf{c} .

5. Approximation theorems

In this section, we prove various approximation results in terms of the parameter κ . Our starting point is the function $U(\kappa)$, which, as we shall see, approximates $u(\kappa)$ in the H^1 seminorm. We will also show that the function

$$W(\kappa) = U(\kappa) - d(\kappa) \tag{52}$$

approximates $w(\kappa)$ in the H^1 norm. Using [Theorem 4.4](#), we can easily verify that this W will be independent of the constants used in the definitions of the functions ψ_i .

We first prove a preliminary lemma, establishing a Poincaré inequality uniform in κ on the domains $\tilde{\Omega}(\kappa)$.

Lemma 5.1. *There exists a constant C independent of κ such that for all $u \in H^1_D(\tilde{\Omega}(\kappa))$, $\kappa \in (0, 1]$,*

$$\|u\|_{0,\tilde{\Omega}} \leq C |\log \kappa|^{\frac{1}{2}} |u|_{1,\tilde{\Omega}}.$$

Proof. It is sufficient to prove the lemma for the case that $\tilde{\Omega}(\kappa)$ is an annulus of inner radius κ and unit outer radius. The general case can then be established from component-wise inequalities.

Let (r, θ) denote the polar coordinates with origin at the center of the annulus. Then, since $u(\kappa, \theta) = 0$,

$$u(r, \theta) = \int_{\kappa}^r \frac{\partial u}{\partial t}(t, \theta) dt,$$

so that by the Schwarz inequality,

$$|u|^2 \leq \left| \int_{\kappa}^r \frac{dt}{t} \right| \left| \int_{\kappa}^r \left(\frac{\partial u}{\partial t} \right)^2 t dt \right| \leq C |\log \kappa| \int_{\kappa}^1 \left(\frac{\partial u}{\partial t} \right)^2 t dt.$$

From this,

$$\int_{\kappa}^1 |u|^2 r dr \leq C \left(\int_{\kappa}^1 r dr \right) |\log \kappa| \int_{\kappa}^1 \left(\frac{\partial u}{\partial t} \right)^2 t dt.$$

Integrating with respect to θ gives the lemma. \square

Turning to the approximation of $w(\kappa)$ by $W(\kappa)$, we note that W satisfies [\(7\)](#) and [\(8\)](#), two of the equations that define w . Although W does not vanish on $\partial\omega$ like w does, it is easy to see that it is $O(\kappa)$ there. Indeed, for $\mathbf{x} \in \partial\omega_i(\kappa)$, $i = 1, 2, \dots, n$, we have, using [\(26\)](#) and [\(30\)](#),

$$W(\kappa)(\mathbf{x}) = \sum_{j=1, j \neq i}^n c_j(\kappa)(\phi_j(\mathbf{x}) - \phi_j(\mathbf{y}_i)) + \sum_{j=1}^n c_j(\kappa)(\psi_j(\mathbf{x}) - \psi_j(\mathbf{y}_i)).$$

Since ϕ_j , $j = 1, 2, \dots, n$, $j \neq i$ and ψ_j , $j = 1, 2, \dots, n$ are all analytic in a neighborhood of $\omega_i(\kappa)$, we can express each of these functions by a Taylor expansion around \mathbf{y}_i to obtain,

$$W(\kappa)(\mathbf{x}) = \sum_{k=1}^m (\kappa\rho_i)^k (A_i^k \cos k\theta_i + B_i^k \sin k\theta_i) + (\kappa\rho_i)^{m+1} \mathcal{R}_i^m(\mathbf{x}), \tag{53}$$

where $\mathbf{x} = (\kappa\rho_i \cos \theta_i, \kappa\rho_i \sin \theta_i) \in \partial\omega_i$. (We use (r_i, θ_i) to denote the polar coordinates centered at \mathbf{y}_i .) The coefficients $A_i^k(\kappa)$, $B_i^k(\kappa)$ will depend on $\mathbf{c}(\kappa)$ and g ; we see using [\(44\)](#) that these coefficients will be uniformly bounded in κ , as will the remainder $\mathcal{R}_i^m(\kappa)(\mathbf{x})$ and its derivatives (which will only be with respect to θ_i , not r_i). For our analysis here, we will set $m = 2$.

Defining the correction term

$$z_i = - \sum_{k=1}^2 \left(\frac{\kappa\rho_i}{r_i} \right)^k (\kappa\rho_i)^k (A_i^k \cos k\theta_i + B_i^k \sin k\theta_i) - (\kappa\rho_i)^3 \mathcal{R}_i^2(\mathbf{x}), \tag{54}$$

we see that

$$W + z_i = 0 \text{ on } \partial\omega_i. \tag{55}$$

Moreover, z_i satisfies the bounds

$$\|z_i\|_{1,\tilde{\Omega}} \leq C\kappa, \quad \|z_i\|_{1,S} \leq C\kappa^2 \tag{56}$$

for any $S \in \mathcal{S}$ (κ small enough).

Since $\partial z_i / \partial n \neq 0$ on $\partial\Omega$, let us next make a modification to these terms. To this end, let $\mathcal{N}_i^1, \mathcal{N}_i^2$ be fixed neighborhoods of \mathbf{y}_i that satisfy $\overline{\mathcal{N}_i^1} \subset \mathcal{N}_i^2 \subset \tilde{\Omega}$, with the distance of \mathcal{N}_i^2 to any other \mathbf{y}_j being positive. Assume κ is small enough so that $\omega_i(\kappa) \subset \mathcal{N}_i^1, \omega_j(\kappa) \subset \tilde{\Omega} \setminus \mathcal{N}_i^2$ for $j \neq i$. Let τ_i be a C^∞ (or suitably smooth) cut-off function which is 1 inside \mathcal{N}_i^1 and 0 outside \mathcal{N}_i^2 . Defining

$$\tilde{z}_i = z_i \tau_i, \tag{57}$$

we see that \tilde{z}_i has the same trace as z_i on $\partial\omega_i$ and hence satisfies (55). Moreover, $\partial\tilde{z}_i / \partial n = 0$ on $\partial\Omega$.

Let us now define

$$Z = \sum_{i=1}^n \tilde{z}_i.$$

Then by the above construction, we have

$$\begin{aligned} \|Z\|_{1,\tilde{\Omega}} &\leq C\kappa, \quad \|Z\|_{1,S} \leq C\kappa^2, \\ \frac{\partial(W+Z)}{\partial n} &= g \text{ on } \partial\Omega, \\ W+Z &= 0 \text{ on } \partial\omega. \end{aligned} \tag{58}$$

However, $W+Z$ is not harmonic on $\tilde{\Omega}$, so we make a further correction to it. We solve the following problem: Find $Y \in H_D^1(\tilde{\Omega})$ satisfying

$$\begin{aligned} -\Delta Y &= \Delta Z \text{ on } \tilde{\Omega} \\ \frac{\partial Y}{\partial n} &= 0 \text{ on } \partial\Omega. \end{aligned} \tag{59}$$

Clearly, the above problem has a unique solution for any $\kappa > 0$. We have the following estimate.

Lemma 5.2. *There exists a constant C independent of $\kappa \in (0, 1]$ such that*

$$\|Y\|_{1,\tilde{\Omega}} \leq C|\log \kappa|^{\frac{1}{2}}\kappa^2.$$

Proof. Using (54), (57), we may write \tilde{z}_i as

$$\begin{aligned} \tilde{z}_i &= -\left(\sum_{k=1}^2 \left(\frac{\kappa\rho_i}{r_i}\right)^k (\kappa\rho_i)^k (A_i^k \cos k\theta_i + B_i^k \sin k\theta_i)\right) \tau_i - ((\kappa\rho_i)^3 \mathcal{R}_i^2(\mathbf{x})) \tau_i \\ &= \tilde{z}_i^1 + \tilde{z}_i^2. \end{aligned}$$

Then \tilde{z}_i^1 is harmonic everywhere on $\tilde{\Omega}$ except for $\mathcal{N}_i^2 \setminus \mathcal{N}_i^1$, so that

$$\|\Delta\tilde{z}_i^1\|_{0,\tilde{\Omega}} = \|\Delta\tilde{z}_i^1\|_{0,\mathcal{N}_i^2 \setminus \mathcal{N}_i^1} \leq C\kappa^2 \tag{60}$$

(where we have used the fact that $\mathcal{N}_i^2 \setminus \mathcal{N}_i^1$ is independent of κ). Also, since $\mathcal{R}_i^2(\mathbf{x})$ is independent of r_i , we can verify that

$$\left\| \frac{\partial^2(\tilde{z}_i^2)}{\partial r_i^2} \right\|_{0,\tilde{\Omega}} \leq C\kappa^3, \quad \left\| \frac{1}{r_i} \frac{\partial(\tilde{z}_i^2)}{\partial r_i} \right\|_{0,\tilde{\Omega}} \leq C\kappa^3, \quad \left\| \frac{1}{r_i^2} \frac{\partial^2(\tilde{z}_i^2)}{\partial \theta_i^2} \right\|_{0,\tilde{\Omega}} \leq C\kappa^2,$$

so that by the polar form of the Laplacian, \tilde{z}_i^2 will also satisfy (60). Hence,

$$\|\Delta Z\|_{0,\tilde{\Omega}} \leq C\kappa^2.$$

We can now bound $|Y|_{1,\tilde{\Omega}}$ by $\|\Delta Z\|_{0,\tilde{\Omega}}$ and use the Poincaré inequality (Lemma 5.1) to get the lemma. \square

We therefore obtain the following theorem.

Theorem 5.3. *Let w be the solution of (7)–(9), and W be defined by (52). Then there exists a constant C independent of $\kappa \in (0, 1]$ such that*

$$\|w - W\|_{1, \tilde{\Omega}} \leq C\kappa. \tag{61}$$

Moreover, for any $S \in \mathcal{S}$, and with κ small enough,

$$\|w - W\|_{1, S} \leq C|\log \kappa|^{\frac{1}{2}}\kappa^2. \tag{62}$$

Proof. With Y, Z defined as above, we see that

$$\begin{aligned} -\Delta(W + Z + Y) &= 0 \text{ on } \tilde{\Omega}, \\ \frac{\partial(W + Z + Y)}{\partial n} &= g \text{ on } \partial\Omega. \end{aligned}$$

Also, $W + Z + Y \in H_D^1(\tilde{\Omega})$, so this sum satisfies (10), the problem that w also satisfies. By uniqueness, we therefore have

$$w = W + Z + Y.$$

The estimates then follow using (58) and Lemma 5.2. \square

Clearly, we will also have the energy norm (seminorm) estimates

$$\|u - U\|_{E, \tilde{\Omega}} = \|w - W\|_{E, \tilde{\Omega}} \leq C\kappa, \tag{63}$$

$$\|u - U\|_{E, S} = \|w - W\|_{E, S} \leq C\kappa^2. \tag{64}$$

Remark 5.1. Suppose we knew the coefficients $A_i^k, B_i^k, k = 1, 2, \dots, m$ in (53). Then we could obtain a higher order approximation W^m to w as follows. Define

$$\begin{aligned} s_i^m &= -\sum_{k=1}^m \left(\frac{\kappa\rho_i}{r_i}\right)^k (\kappa\rho_i)^k (A_i^k \cos k\theta_i + B_i^k \sin k\theta_i), \\ W^m &= W + \sum_{i=1}^n s_i^m \tau_i, \end{aligned}$$

where τ_i is a suitable cut-off function like the one in (57). Then the steps leading to Theorem 5.3 easily show that

$$\begin{aligned} \|w - W^m\|_{1, \tilde{\Omega}} &\leq C\kappa^{m+1}, \\ \|w - W^m\|_{1, S} &\leq C|\log \kappa|^{\frac{1}{2}}\kappa^{m+2}. \end{aligned}$$

This can be the basis for designing a higher-order extension of our method which depends on recovering approximations to A_i^k, B_i^k .

Let us now prove a result for the asymptotic limit to the solution $u(\kappa)$ as $\kappa \rightarrow 0$. As explained in Section 2, the limit of $w(\kappa)$ will not exist as an $L_2(\Omega)$ function, but the limit of $u(\kappa)$ will. Although the energy norm of this limit u_0 will not be finite, both $w(\kappa)$ and $u(\kappa)$ will converge to u_0 in $\|\cdot\|_{E, S}$ (i.e. the $H^1(S)$ seminorm) for any fixed $S \in \mathcal{S}$.

Theorem 5.4. *There exists a unique $u_0 \in L_2(\Omega)$ such that $\forall S \in \mathcal{S}, u_0 \in \mathcal{E}(S)$ and*

$$\|w(\kappa) - u_0\|_{E, S} = \|u(\kappa) - u_0\|_{E, S} \leq C|\log \kappa|^{-1}$$

with C a constant independent of κ , but dependent on S .

Proof. Noting (26) and the limiting formula (46), we define

$$u_0 = U(0) = \sum_{i=1}^n c_i(0)(\phi_i + \psi_i) = \sum_{i=1}^n \left(\frac{G}{2\pi n}\right)(\phi_i + \psi_i).$$

Although ϕ_i is undefined at \mathbf{y}_i , it belongs to $L_2(\Omega)$, so that $u_0 \in L_2(\Omega)$. Also, since $W(\kappa)$ and $U(\kappa)$ differ only by a constant,

$$\|w(\kappa) - u_0\|_{E,S} = \|u(\kappa) - u_0\|_{E,S} \leq \|w(\kappa) - W(\kappa)\|_{E,S} + \|U(\kappa) - U(0)\|_{E,S}.$$

The first term above is bounded by $C\kappa^2$ by (64). For the second term, we note that

$$\|U(\kappa) - U(0)\|_{E,S} = \left\| \sum_{i=1}^n (c_i(\kappa) - c_i(0))(\phi_i + \psi_i) \right\|_{E,S}.$$

Since ϕ_i, ψ_i are analytic and bounded (independently of κ) in any norm on S , the theorem follows by (45). \square

Let us now turn to the determination of the forces q_i defined in (12). We will approximate them by the quantities

$$Q_i = \int_{\partial\omega_i} \frac{\partial U}{\partial n} ds. \tag{65}$$

Since all the terms in (26) are harmonic over ω_i except for ϕ_i , this reduces to

$$Q_i = c_i \int_{\partial\omega_i} \frac{\partial \phi_i}{\partial n} ds.$$

Noting that

$$\frac{\partial \phi_i}{\partial n} = -\frac{1}{\sigma_i} \text{ on } \partial\omega_i,$$

we have the following identity.

$$Q_i = -2\pi c_i. \tag{66}$$

Hence, the coefficients c_i are simply scaled approximations to the forces q_i . We obtain the following estimate.

Theorem 5.5. *Let q_i, Q_i be defined by (12), (65) respectively. Then there exists a constant C , independent of $\kappa \in (0, 1]$, such that*

$$|q_i(\kappa) - Q_i(\kappa)| \leq C\kappa^2.$$

Proof. Let $A \subset \tilde{\Omega}$ be an annulus with center \mathbf{y}_i , of thickness $O(1)$ and distance $O(1)$ away from $\partial\omega$. Suppose ∂A is any concentric circle in this annulus. Since u, U are both harmonic on $\tilde{\Omega}$, we have

$$\begin{aligned} q_i - Q_i &= \int_{\partial\omega_i} \frac{\partial(u - U)}{\partial n} ds \\ &= - \int_{\partial A} \frac{\partial(u - U)}{\partial n} ds. \end{aligned}$$

Integrating over all such circles ∂A through the thickness of A , we see that

$$\begin{aligned} |q_i - Q_i| &= \frac{1}{\text{meas}(A)} \left| \int_A \frac{\partial(u - U)}{\partial n} d\mathbf{x} \right| \\ &\leq \frac{1}{(\text{meas}(A))^{\frac{1}{2}}} |u - U|_{1,A} \end{aligned}$$

where we have used Schwarz’s inequality. Since A is bounded away from the holes, the theorem follows from (64). \square

From the above and Theorem 4.4, we see that

$$q_i(0) = Q_i(0) = -2\pi c_i(0) = -\frac{G}{n}. \tag{67}$$

Denoting $q_i(0)$ by q_i^0 , and using (67), (45), we have the following analog to Theorem 5.4, for our other QoI, the forces.

Theorem 5.6. For each $i = 1, 2, \dots, n$, there exists a unique q_i^0 defined by (67) such that

$$|q_i(\kappa) - q_i^0| \leq C |\log \kappa|^{-1} \tag{68}$$

with C a constant independent of κ .

Remark 5.2. The slow $O(|\log \kappa|^{-1})$ convergence in Theorems 5.4 and 5.6 has to be taken into consideration when the asymptotic limit is sometimes used in engineering. As shown by Theorems 5.3 and 5.5, we get much higher accuracy when we use the solution $W(\kappa)$ or coefficients $c_i(\kappa)$. In particular, (67) shows the QoI q_i tend to limits that are the same for all i , but this convergence is only logarithmic. For $\kappa > 0$ of practical interest, the approximations given by $Q_i(\kappa)$ in (66) can give dramatically different (and much more accurate) results. See the example with two unequal holes in Section 7.

6. Modified finite element approximation

Instead of directly approximating the entire solution w , our modified FEM consists of approximating only the components ψ_i over the domain Ω . Let $V_h \subset \Omega$ be a FE subspace, and define $\psi_{i,h} \in V_h$ by

$$B_{\Omega}(\psi_{i,h}, v) = \int_{\partial\Omega} \left(\frac{2\pi}{G} g - \frac{\partial\phi_i}{\partial n} \right) v \, ds \quad \forall v \in V_h, \tag{69}$$

$$\int_{\Omega} \psi_{i,h}(\mathbf{x}) \, d\mathbf{x} = 0. \tag{70}$$

Here, (70) may be replaced by a more convenient condition to fix the constant in $\psi_{i,h}$, e.g. by using a point constraint $\psi_{i,h}(\mathbf{x}_0) = 0$, as is commonly done in the FEM for pure Neumann conditions (and as we do in Section 7). Note that (69)–(70) is independent of κ and does not involve meshing the holes. Hence, the same FE matrices can be (inexpensively) used to solve each of these n problems, for each value of κ that might be of interest.

The usual FE theory shows that $\psi_{i,h}$ will be the best approximation in V_h to ψ_i in the energy norm. For V_h given by continuous piecewise polynomials of degree $p \geq 1$ on a suitably regular mesh (of triangles or rectangles) with mesh size h , we obtain the standard estimate,

$$\|\psi_i - \psi_{i,h}\|_{1,\Omega} \leq Ch^{\min(p,k-1)} \|\psi_i\|_{k,\Omega}. \tag{71}$$

As mentioned earlier, the function ϕ_i , which appears as data in (69), will be smooth except in the vicinity of \mathbf{y}_i . Assuming g and Ω are smooth enough to give $\psi_i \in H^k(\Omega)$ with $k \geq p + 1$, (71) becomes

$$\|\psi_i - \psi_{i,h}\|_{1,\Omega} \leq Ch^p. \tag{72}$$

Under suitable regularity assumptions on the data, boundary of the domain and meshes (which we assume in all the results below), one also obtains [30]:

$$\|\psi_i - \psi_{i,h}\|_{\infty,\Omega} \leq C |\log h|^s h^{p+1}, \tag{73}$$

where $s = 1$ for $p = 1$ and is 0 otherwise.

Remark 6.1. Since ψ_i is smooth, the p version [31] will give particularly high convergence rates. For instance, instead of (72), we will have

$$\|\psi_i - \psi_{i,p}\|_{1,\Omega} \leq Cp^{-(k-1)},$$

i.e. the order of convergence is only bounded by the smoothness of ψ_i (which may be limited e.g. due to corners in the domain). For ψ_i of unlimited smoothness, the rate will be exponential.

We now define $(\mathbf{c}_h(\kappa), d_h(\kappa))$ by the analogs of (27), (30) used to define $(\mathbf{c}(\kappa), d(\kappa))$:

$$\sum_{i=1}^n c_{i,h}(\kappa) = \frac{G}{2\pi}. \tag{74}$$

$$c_{i,h}(\kappa) \log \sigma_i(\kappa) + \sum_{j=1, j \neq i}^n c_{j,h}(\kappa) \phi_j(\mathbf{y}_i) + \sum_{j=1}^n c_{j,h}(\kappa) \psi_{j,h}(\mathbf{y}_i) = d_h(\kappa), \quad i = 1, 2, \dots, n. \tag{75}$$

Then (32) defines an approximation B_h to matrix B . The L_∞ estimate (73) shows that

$$\|B - B_h\| \leq C|\log h|^s h^p. \tag{76}$$

Since the exact functions ϕ_i are retained in the FE computation, the matrix D remains unchanged.

Let B_h satisfy (35), i.e.

$$\alpha_h = \frac{\|B_h\|}{|\log R|} < \frac{1}{2}. \tag{77}$$

(By (76), this will certainly hold for h small enough.) Then the analogs of Lemmas 4.1–4.3 and Theorem 4.4 all hold (with $M_h = D + B_h$ and Z_h defined analogously to Z). We obtain the following result.

Theorem 6.1. *Suppose h, R are such that condition (77) holds. Then Eqs. (74), (75) have a unique solution for any $\kappa \in (0, 1]$. Moreover, there exists a constant C independent of κ, h such that*

$$\|\mathbf{c}(\kappa) - \mathbf{c}_h(\kappa)\| \leq C|\log \kappa|^{-1}|\log h|^s h^p, \tag{78}$$

$$|d(\kappa) - d_h(\kappa)| \leq C|\log h|^s h^p. \tag{79}$$

Proof. Using expansion (39) for Z, Z_h we see that

$$Z - Z_h = -(B - B_h)D^{-1}(I - (B - B_h)D^{-1} + ((B - B_h)D^{-1})^2 - \dots),$$

from which, analogously to (40),

$$\|Z - Z_h\| \leq C|\log h|^s h^p \min\{1, |\log R||\log \kappa|^{-1}\}.$$

Hence, for κ small enough,

$$\|M^{-1} - M_h^{-1}\| = \|D^{-1}(Z - Z_h)\| \leq C|\log \kappa|^{-2}|\log h|^s h^p.$$

Using (50), we have

$$\mathbf{c} - \mathbf{c}_h = \left(\frac{M^{-1}\mathbf{e}}{\mathbf{e}^T M^{-1}\mathbf{e}} - \frac{M_h^{-1}\mathbf{e}}{\mathbf{e}^T M_h^{-1}\mathbf{e}} \right) \frac{G}{2\pi}.$$

Estimate (78) is easily established from this. Also, (79) can be established from the relation

$$d - d_h = \left(\frac{1}{\mathbf{e}^T M^{-1}\mathbf{e}} - \frac{1}{\mathbf{e}^T M_h^{-1}\mathbf{e}} \right) \frac{G}{2\pi}. \quad \square$$

Remark 6.2. The extra $|\log \kappa|^{-1}$ term in (78) is consistent with the fact that for fixed h , if $\kappa \rightarrow 0$, then both $\mathbf{c}(\kappa)$ and $\mathbf{c}_h(\kappa)$ converge to the same limit $\mathbf{c}(0)$ at rate $O(|\log \kappa|^{-1})$, as in (45).

Let us now define $U_h(\kappa), W_h(\kappa)$ by

$$U_h(\kappa) = \sum_{i=1}^n c_{i,h}(\kappa)(\phi_i + \psi_{i,h}), \quad W_h(\kappa) = U_h(\kappa) - d_h(\kappa). \tag{80}$$

Then, for any $\kappa \in (0, 1]$,

$$W(\kappa) - W_h(\kappa) = \sum_{i=1}^n (c_i - c_{i,h})(\kappa)(\phi_i + \psi_i) + \sum_{i=1}^n c_{i,h}(\kappa)(\psi_i - \psi_{i,h}) - (d(\kappa) - d_h(\kappa)).$$

Using (72) and Theorem 6.1, this gives

$$\|W(\kappa) - W_h(\kappa)\|_{1, \tilde{\Omega}} \leq C|\log h|^s h^p, \tag{81}$$

with C a constant independent of κ . Combining this with the estimates for $w(\kappa) - W(\kappa)$, we have the following theorem.

Theorem 6.2. *There exists a constant C independent of $\kappa \in (0, 1]$ and h such that*

$$\|w(\kappa) - W_h(\kappa)\|_{1, \tilde{\Omega}} \leq C(\kappa + |\log h|^s h^p). \tag{82}$$

Moreover, for any $S \in \mathcal{S}$, and with κ small enough,

$$\|w(\kappa) - W_h(\kappa)\|_{1, S} \leq C(|\log \kappa|^{\frac{1}{2}} \kappa^2 + |\log h|^s h^p). \tag{83}$$

Corollary 6.2.1. *For any $S \in \mathcal{S}$, the energy can be approximated by $E(W_h(\kappa), S)$, where*

$$|E(w(\kappa), S) - E(W_h(\kappa), S)| \leq C(|\log \kappa| \kappa^4 + |\log h|^{2s} h^{2p}).$$

Finally, we also can use the coefficients $c_{i,h}$ to define approximations to our other QoI, the forces q_i , by

$$Q_{i,h} = -2\pi c_{i,h}. \tag{84}$$

Then [Theorem 5.5](#) together with [\(78\)](#) gives the following result.

Theorem 6.3. *There exists a constant C , independent of $\kappa \in (0, 1]$ and h such that*

$$|q_i(\kappa) - Q_{i,h}(\kappa)| \leq C(\kappa^2 + |\log \kappa|^{-1} |\log h|^s h^p).$$

Remark 6.3. Note that we could also define other approximations to q_i , for instance,

$$\tilde{Q}_{i,h} = \int_{\partial\omega_i} \frac{\partial U_h}{\partial n} ds, \tag{85}$$

or, for that matter, the integral over any other contour around ω_i contained in Ω which does not include or intersect the other holes. For U , all these definitions give exactly the same value, since U is harmonic. For U_h , which is only approximately harmonic, these do not have to be equal; however, we verify in the next section that the difference using [\(84\)](#) and [\(85\)](#) is negligible.

7. Computational results for modified FEM

In this section, we report the results of some computational experiments performed with our modified FEM. Although our estimates are asymptotic in nature, problems of practical interest will often have holes with only moderately small radii (relative to the dimension of the domain). It is therefore particularly relevant to obtain insight on the range of practical parameters for which our method will be accurate.

We take $g = 1$ and consider the case of two holes on the square domain $\Omega = (-1, 1)^2$. Initially, we assume the holes are of equal radius, $\sigma_1(\kappa) = \sigma_2(\kappa) = \kappa < \frac{1}{2}$, with centers located at $\mathbf{y}_1 = (0, 0)$ and $\mathbf{y}_2 = (\frac{1}{2}, 0)$.

The locations of these centers (but not the radii) determine the two logarithmic singularities ϕ_1 and ϕ_2 which we incorporate in our calculations. We then use a uniform rectangular mesh of mesh size h on the entire domain Ω (without the holes) to compute finite element approximations to the unknown functions ψ_1 and ψ_2 . (Instead of condition [\(25\)](#), we set $\psi_i(-1, -1) = 0$.) We use both bilinear ($p = 1$) and biquadratic ($p = 2$) elements. The radii only appear in the calculations while solving the linear system [\(74\)](#), [\(75\)](#), leading to our approximate solution W_h given by [\(80\)](#).

Since the exact solution w for this problem is unknown, we compare our results with a full-blown FE solution to [\(7\)–\(9\)](#), posed over the domain $\tilde{\Omega}$ (this time with modeling of the holes included). We use the Matlab PDE Toolbox code, which employs automatic meshing with linear triangular elements. We set the refinement successfullly higher until our results do not change significantly, indicating a level of accuracy high enough to make the comparison.

Define S_κ to be the region Ω with squares of side 2κ and centers $\mathbf{y}_1, \mathbf{y}_2$ removed, and denote $S = S_{1/8} (= [-1, 1]^2 \setminus (([-\frac{1}{8}, \frac{1}{8}]^2 \cup [\frac{3}{8}, \frac{5}{8}] \times [-\frac{1}{8}, \frac{1}{8}]))$ ([Fig. 3](#)). We first fix $\kappa = 1/32$ and calculate the relative error for $\|w - W_h\|_{E,S}$ with decreasing h (where w is our PDE Toolbox solution described above) using bilinear ($p = 1$) elements for W_h .

Looking at the ratio of errors with successive mesh sizes h in [Table 1](#), we observe the decrease is close to $O(h)$. Our interpretation is that the error in κ is much smaller than the error in h for this choice of parameters, and we are already observing the asymptotic FE rate predicted by the last term in [\(83\)](#).

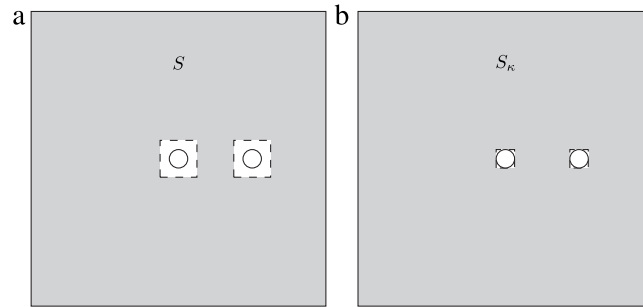


Fig. 3. S and S_κ for $\kappa = 1/16$.

Table 1

Relative error for $\|w - W_h\|_{E,S}$ with $\kappa = 1/32$, $p = 1$.

h	$\frac{\ w - W_h\ _{E,S}}{\ w\ _{E,S}}$ (%)	Ratio
1/16	6.01	
1/32	3.08	1.95
1/64	1.68	1.83

Table 2

Relative error for $\|W - W_h\|_{E,S}$ with $\kappa = 1/32$, $p = 2$.

h	$\frac{\ W - W_h\ _{E,S}}{\ W\ _{E,S}}$ (%)	Ratio
1/8	0.0512	
1/16	0.0129	3.97
1/32	0.0032	4.03
1/64	0.0008	4.00

Table 3

Relative error for $\|w - W_h\|_{E,S}$ with different κ , $p = 2$, $h = 1/128$.

κ	$\frac{\ w - W_h\ _{E,S}}{\ w\ _{E,S}}$ (%)	Ratio
1/8	8.49	
1/16	2.21	3.84
1/32	0.59	3.74

For *biquadratic* elements, it is difficult to get the error term involving κ in (83) small enough to make the error due to h dominate. So we instead investigate the convergence (81) (over S instead of $\tilde{\Omega}$) of the approximations $W_h(\kappa)$ to $W(\kappa)$ where κ is kept fixed at $1/32$. Since we do not have an exact $W(\kappa)$, we use $W = W_{1/256}(\kappa)$ (i.e. h taken very small) in Table 2.

The numbers in Table 2 show we are in the asymptotic $O(h^p)$ range ($p = 2$) for the finite element approximation, which is expected from (81). (We remark that a comparison between $W_{1/256}$ and W_h for bilinears shows results very similar to those in Table 1.)

Let us now try to isolate the dependence on κ . For Tables 3 and 4, we choose our mesh size h so that decreasing it further does not significantly change W_h for the κ in the table. Since the convergence is much faster with biquadratics, we only use those.

We see from Table 3 that the errors decrease at almost an $O(\kappa^2)$ rate, suggesting we are already in the asymptotic range of the estimate (83) as far as κ goes. (Here, the $O(h^2)$ FE error is small enough to be negligible.)

Theorem 6.2 also suggests that if we measure the error over all of $\tilde{\Omega}$ rather than just a fixed domain S , then the convergence will be only $O(\kappa)$. To investigate this effect, for each κ above, we compute $\|w - W_h\|_{E,S_\kappa}$ (with h small enough). Note that S_κ contains the smallest square holes that can be circumscribed around the circular holes. Since our mesh is rectangular, this domain, which we expect to behave similarly to $\tilde{\Omega}$, is easier to work with.

Table 4

Relative error for $\|w - W_h\|_{E,S_\kappa}$ with different κ , $p = 2$, $h = 1/128$.

κ	$\frac{\ w - W_h\ _{E,S_\kappa}}{\ w\ _{E,S_\kappa}}$ (%)	Ratio
1/8	8.49	
1/16	4.00	2.12
1/32	1.92	2.08

Table 5

Difference in computed forces, first and second holes, $p = 2$, $h = 1/512$.

κ	$Q_{1,h}$	$ Q_{1,h} - \tilde{Q}_{1,h} $	$Q_{2,h}$	$ Q_{2,h} - \tilde{Q}_{2,h} $
1/8	-4.3154	3.0999e-07	-3.6845	1.0125e-07
1/16	-4.2158	1.9599e-08	-3.7841	4.2399e-08
1/32	-4.1640	1.3001e-09	-3.8359	3.5001e-09
1/64	-4.1322	1.0101e-10	-3.8677	7.8201e-10

Table 6

Relative error in computed forces, first and second hole, $p = 2$, $h = 1/512$.

κ	$\frac{ q_1 - Q_{1,h} }{ q_1 }$ (%)	Ratio	$\frac{ q_2 - Q_{2,h} }{ q_2 }$ (%)	Ratio
1/8	0.67		0.79	
1/16	0.15	4.47	0.11	7.18
1/32	0.04	3.75	0.03	3.67

Table 7

Relative error in computed forces, first and second hole (unequal), $p = 2$, $h = 1/512$.

κ	$Q_{1,h}$	$\frac{ q_1 - Q_{1,h} }{ q_1 }$ (%)	Ratio	$Q_{2,h}$	$\frac{ q_2 - Q_{2,h} }{ q_2 }$ (%)	Ratio
1/4	-5.9487	2.03		-2.0513	5.19	
1/8	-5.4671	0.52	3.90	-2.5329	1.01	5.14
1/16	-5.1764	0.11	4.73	-2.8236	0.21	4.81
1/32	-4.9818	0.02	5.50	-3.0182	0.05	4.20

Table 4 shows that the order of convergence indeed decreases to $O(\kappa)$ when we measure the error up to the holes. This is consistent with the estimate (82).

Next, we report some results on the computation of the forces on the hole boundaries. Once again, we use biquadratic elements with sufficiently small mesh size ($h = 1/512$) to try and isolate the effects due to κ .

First, we demonstrate in Table 5 that the values $Q_{i,h}$ obtained using (84) closely match the values $\tilde{Q}_{i,h}$ from (85) (see Remark 6.3).

From Table 5, we may also observe that $Q_{1,h}, Q_{2,h}$ both approach their common limiting value of $q_i^0 = -4$ at a rate of $O(|\log \kappa|^{-1})$ as $\kappa \rightarrow 0$. This is consistent with Remark 6.2. (Note that since $g = 1$, the total force G over the boundary of the square is 8, and in the limit, this gets equally distributed over the holes, as per Eq. (67).)

Next, Table 6 shows the error between the “exact” force q_i calculated using the PDE Toolbox solution, and our computed approximations $Q_{i,h}$ (with $h = 1/512$).

We see that the ratios vary, but their average, 4.57, is consistent with quadratic convergence in κ .

Let us also consider a case of unequal holes, where the first hole’s radius is four times the second’s. The centers are now at $\mathbf{y}_1 = (0, 0)$ and $\mathbf{y}_2 = (3/4, 0)$, with $\sigma_1 = \kappa, \sigma_2 = \kappa/4$. As Table 7 shows, the forces are now much more unequally distributed, as can be expected from physical intuition (with the larger support having a greater force). Note that both forces are still converging to their common limiting value $q_i^0 = -4$, but only logarithmically. This indicates that the asymptotic limit of -4 may not be a valid approximation in practical situations (as pointed out in Remark 5.2). The relative error using the value of $q_2^0 = -4$ for the force on the second hole would be about 33% for $\kappa = 1/32$ and 95% for $\kappa = 1/4$.

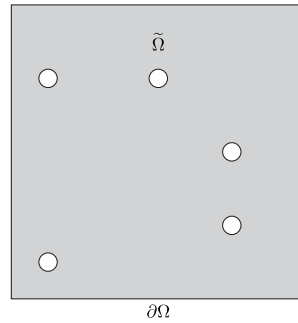


Fig. 4. Domain with five holes.

Table 8

Relative error for $\|w - W_h\|_{E,S}$ with $\kappa = 1/32$, $p = 2$ (five holes).

h	$\frac{\ w - W_h\ _{E,S}}{\ w\ _{E,S}}$ (%)	Ratio
1/16	6.55	
1/32	3.34	2.13
1/64	1.82	2.16

Table 9

Relative error for $\|w - W_h\|_{E,S}$ with different κ , $p = 2$, $h = 1/128$ (five holes).

κ	$\frac{\ w - W_h\ _{E,S}}{\ w\ _{E,S}}$ (%)	Ratio
1/8	12.46	
1/16	3.32	3.75
1/32	0.91	3.65

Table 7 also shows that the errors are comparable to the case of equal holes. Moreover, the values of κ used already display the asymptotic convergence rate of about $O(\kappa^2)$ for the error. Let us remark that the energy norm errors (not shown here) behave as expected, i.e. we see similar convergence rates in h and κ as those reported earlier for the case of equal holes.

Remark 7.1. We can also expect the distribution of the forces to be unbalanced when the radii are equal, but one hole is much closer to the boundary than the other. Again, the asymptotic limit may yield an unsatisfactory approximation to cases where $\kappa > 0$, but this will be less of a problem as $\kappa \rightarrow 0$, since the distance to the boundary relative to κ will then increase and become comparable.

As a final test, we consider the case of five equal circular holes, with centers at $\mathbf{y}_1 = (0, \frac{1}{2})$, $\mathbf{y}_2 = (\frac{1}{2}, 0)$, $\mathbf{y}_3 = (-\frac{3}{4}, -\frac{3}{4})$, $\mathbf{y}_4 = (\frac{1}{2}, -\frac{1}{2})$, $\mathbf{y}_5 = (-\frac{3}{4}, \frac{1}{2})$ (Fig. 4). Define S_κ to be the region Ω with squares of side 2κ and centers \mathbf{y}_i , $i = 1, \dots, 5$, removed and denote $S = S_{1/8}$.

We first fix $\kappa = 1/32$ and calculate the relative error for $\|w - W_h\|_{E,S}$ with decreasing h (where w is our PDE Toolbox solution described above) using bilinear ($p = 1$) elements for W_h . We observe the expected $O(h)$ convergence rate (see Table 8).

As we did for two holes, we now try to isolate the dependence on κ . For Tables 9 and 10, we choose our mesh size h so that decreasing it further does not significantly change W_h for the κ in the table. We use biquadratics for their rapid convergence.

We see that the behavior of both $\|w - W_h\|_{E,S}$ and $\|w - W_h\|_{E,S_\kappa}$ is consistent with the asymptotic theory.

Next, let us report results for the computation of the forces. We use biquadratic elements with sufficiently small mesh size ($h = 1/256$) to try and isolate the effects due to κ . Note that the asymptotic limiting value is now $q_i^0 = -1.6$.

Table 10

Relative error for $\|w - W_h\|_{E, S_\kappa}$ with different κ , $p = 2$, $h = 1/128$ (five holes).

κ	$\frac{\ w - W_h\ _{E, S_\kappa}}{\ w\ _{E, S_\kappa}}$ (%)	Ratio
1/8	12.46	
1/16	5.84	1.85
1/32	2.70	1.95

Table 11

Computed force, $p = 2$, $h = 1/256$ (five holes).

κ	$Q_{1,h}$	$Q_{2,h}$	$Q_{3,h}$	$Q_{4,h}$	$Q_{5,h}$
1/8	-1.4872	-1.3363	-1.7013	-1.7540	-1.7212
1/16	-1.5040	-1.4073	-1.6934	-1.6990	-1.6962
1/32	-1.5178	-1.4460	-1.6853	-1.6710	-1.6798

Table 12

Relative error in computed force, $p = 2$, $h = 1/256$ (five holes).

k	$\frac{ q_1 - Q_{1,h} }{ q_1 }$ (%)	$\frac{ q_2 - Q_{2,h} }{ q_2 }$ (%)	$\frac{ q_3 - Q_{3,h} }{ q_3 }$ (%)	$\frac{ q_4 - Q_{4,h} }{ q_4 }$ (%)	$\frac{ q_5 - Q_{5,h} }{ q_5 }$ (%)
1/8	0.71	1.59	0.94	0.98	0.55
1/16	0.13	0.35	0.22	0.20	0.13
1/32	0.0007	0.08	0.04	0.07	0.01

Table 11 shows a maximum error of about 20% (hole 2, $\kappa = 1/8$) if the asymptotic value of -1.6 is used as an approximation. This, of course, will vary depending on the value of κ and the placement of the holes.

Table 12 shows that the computations are consistent with the expected asymptotic convergence estimate of $O(\kappa^2)$. Our experiments therefore support the robustness of the method with respect to the number of holes.

8. FE computations for the intuitive model

We now return to the ill-posed Intuitive Model (1), (2), (6) described in the introduction (with $K = 1$). This model follows from the “natural” assumption that since the radii σ_i of the discs are small, the membrane can be regarded as being supported only at the single points \mathbf{y}_i . As already stated, this model is incorrect, since the PDE is of second order, and therefore cannot have point boundary constraints for a two- or higher-dimensional domain. Thus, the model has no solution in the energy space $\mathcal{E}(\Omega)$. Nevertheless, we can still apply the classical FEM to this model to obtain a finite-dimensional “approximation” w_h defined as follows.

As in Section 6, let $V_h \subset \Omega$ be a conforming FE subspace of continuous piecewise polynomials of degree $p \geq 1$ on a mesh of triangles or rectangles on Ω . For simplicity we assume the space is defined in terms of nodal basis functions, and each \mathbf{y}_i coincides with a node. Define $V_h^0 = \{v \in V_h, v(\mathbf{y}_i) = 0, i = 1, 2, \dots, n\}$. Then we seek $w_h \in V_h^0$ satisfying

$$B_\Omega(w_h, v) = \int_{\partial\Omega} g v \, ds \quad \forall v \in V_h^0. \tag{86}$$

The constraints on V_h^0 ensure the existence of a unique solution w_h . An approximate QoI $E(w_h, S)$ can be immediately calculated from this.

To determine an approximation for the other QoI, we define

$$Q_{i,h}^0 = B_\Omega(w_h, \eta_i), \tag{87}$$

where $\eta_i \in V_h$ is the nodal basis function that is 1 at \mathbf{y}_i and vanishes at other nodes. Then it is easily verified that for all $v \in V_h$,

$$B_\Omega(w_h, v) = \sum_{i=1}^n Q_{i,h}^0 v(\mathbf{y}_i) + \int_{\partial\Omega} g v \, ds. \tag{88}$$

Table 13Estimated relative error in energy, $p = 1$ (Intuitive Model, $\kappa = 0$).

h	E_h^0	$\frac{ E_h^0 - E_{h/2}^0 }{ E_{h/2}^0 }$ (%)
1/16	15.5425	0.54
1/32	15.6273	0.13
1/64	15.6483	0.04
1/128	15.6548	0.02
1/256	15.6575	

Table 14Estimated relative error in energy, $p = 1$ (Basic Model, $\kappa = 1/32$).

h	E_h^κ	$\frac{ E_h^\kappa - E_{h/2}^\kappa }{ E_{h/2}^\kappa }$ (%)
1/16	15.5769	0.30
1/32	15.6245	0.08
1/64	15.6367	0.02
1/128	15.6379	0.01
1/256	15.6405	

Substituting $v = 1$ in (88) leads to the required condition

$$\sum_{i=1}^n Q_{i,h}^0 = -G.$$

Let us mention that for actual implementation, $Q_{i,h}^0$ can be easily recovered from w_h using the full stiffness matrix corresponding to the form $B_\Omega(\cdot, \cdot)$ over V_h .

We now present the results of some computations with the above FE method based on the Intuitive Model. We take $\Omega = (-1, 1)^2$ with holes centered at $\mathbf{y}_1 = (0, 0)$ and $\mathbf{y}_2 = (\frac{1}{2}, 0)$ (Fig. 3) and let the hole radii $\sigma_1 = \sigma_2 = \kappa = 0$. We let $g = 1$ as in Section 7, and use bilinear finite elements on a uniform mesh of rectangles. Since we do not know the exact value of the first QoI, the energy, we estimate the relative error in energy via the usual computational technique of comparing $E_h^0 = E(w_h, S)$ and $E_{h/2}^0 = E(w_{h/2}, S)$. Here, $S = [-1, 1]^2 \setminus ([-\frac{1}{8}, \frac{1}{8}]^2 \cup [\frac{3}{8}, \frac{5}{8}] \times [-\frac{1}{8}, \frac{1}{8}])$.

We observe from Table 13 that the estimated error is extremely small, and moreover decreases comparably to the $O(h^2)$ rate expected with bilinear elements (in the spirit of Corollary 6.2.1). From the standpoint of engineering assessment, the value of E_h^0 would be regarded to have converged.

Is the above convergence test reliable? To assess this, we perform the same test for the case of holes with finite radius $\sigma_1 = \sigma_2 = \kappa = 1/32$. The resulting values, shown in Table 14, are computed using the modified FEM on the Basic Model. We observe similar $O(h^2)$ convergence, and also see that the value of the energy over S for the two cases is close. Since we have theoretically established the convergence in the case of the Basic Model, we know the computed values for E_h^κ in Table 14 are accurate, suggesting the test is reliable. So with this reassurance, we can conclude that the test shown in Table 13 is reliable as well, and the values for E_h^0 are, indeed, converging to the asymptotic value of our energy QoI.

We now compute our second QoI $Q_{i,h}^0$, using the Intuitive Model as explained above. Once again, we estimate the relative error by comparing $Q_{i,h}^0$ with $Q_{i,h/2}^0$. Columns 3 and 6 of Table 15 show this error as being extremely small (though decreasing much slower than $O(h)$), leading us again to the conclusion that our computed values have converged. Moreover, the fact that the sum of the computed forces equals -8 , and hence satisfies an equilibrium check, might give us additional confidence in our results.

The question the above tests for convergence do not answer, however, is *what* we have converged to. For instance, if we are performing calculations on this limiting Intuitive Model hoping to get good approximations for the case $\kappa = 1/4$ and unequal holes discussed in the previous section (see Table 7), then our recovered value of $Q_{2,h}^0$ above is about *twice* the actual desired value, leading to a relative error of almost 100%. Even for $\kappa = 1/32$, our relative error is about 33%. This shows the danger in relying solely on convergence tests and other numerical checks.

Instead, an understanding of the underlying analytic situation is needed to correctly interpret the above results. This includes an awareness that at best, we should expect the Intuitive Model to only yield an approximation to the

Table 15

Estimated and exact relative errors in forces, $p = 1$ (Intuitive Model, $\kappa = 0$).

h	$Q_{1,h}^0$	$\frac{ Q_{1,h}^0 - Q_{1,h/2}^0 }{ Q_{1,h/2}^0 }$ (%)	$\frac{ Q_{1,h}^0 - q_1^0 }{ q_1^0 }$ (%)	$Q_{2,h}^0$	$\frac{ Q_{2,h}^0 - Q_{2,h/2}^0 }{ Q_{2,h/2}^0 }$ (%)	$\frac{ Q_{2,h}^0 - q_2^0 }{ q_2^0 }$ (%)
1/16	-4.1085	0.36	2.71	-3.8915	0.38	2.71
1/32	-4.0937	0.28	2.34	-3.9063	0.29	2.34
1/64	-4.0824	0.22	2.06	-3.9176	0.22	2.06
1/128	-4.0736	0.18	1.84	-3.9264	0.18	1.84
1/256	-4.0664		1.66	-3.9336		1.66

asymptotic limits of our QoI, which (as discussed in the previous section) may or may not be close to the values for $\kappa > 0$. With deeper analysis comes the knowledge that in the limiting case the forces are distributed equally (no matter what the relative sizes of the actual holes are in reality). Using this, one can calculate the exact error, as we have done in columns 4 and 7 of Table 15. These show that each $Q_{i,h}^0$ does, indeed, appear to be converging to its asymptotic limit, but the true error is about ten times as large as the estimated one.

Columns 4 and 7 also indicate that the observed convergence in h is very slow ($O(|\log h|^{-1})$ at best). In fact, there is no guarantee that QoI obtained from discretizing the Intuitive Model will converge to the expected asymptotic limits (or at all). As computational results in Section 17.1 of [8] for the related lug problem from elasticity show, the intuitive FE solution can be completely mesh dependent. One reason that our results in Tables 13 and 15 are so well-behaved is that we have taken a uniform mesh. For such meshes, it is known (see e.g. [32]) that the finite element approximation of problems like (21) with delta functions as data satisfy $\|\phi_i - \phi_{i,h}\|_{0,\Omega} \leq Ch$. (Such problems are what we essentially end up solving due to the presence of terms $v(\mathbf{y}_i)$ in (88) derived from point constraints.) If, instead, we refined the mesh only in the vicinity of one hole, we would capture the logarithmic singularity there much better, skewing the results.

In this connection, let us remark that in addition to its ill-posedness, the Intuitive Model has the further disadvantage of being the “natural” limiting case for several different scenarios. One such scenario is the case we considered in Remark 4.2, where the holes converged to 0 at unequal rates. This gives rise to a different limiting distribution of forces (51), which, arguably, is an equally valid candidate for the intuitive FE discretizations to converge to. Perhaps with an appropriately designed mesh, they would.

Our conclusion is therefore that the Intuitive Model should be used with much caution, and only with substantial analytic understanding of the underlying problem. Let us add that our discussion has only related to the verification aspect of the modeling, and not the validation aspect. The latter would include, for instance, the uncertainty in the QoI due to a large gradient in the solution or due to the type of membrane. Often, verification and validation are only performed for simple cases, and this can be very misleading.

9. Summary and conclusions

This paper addresses the problem of determining two quantities of interest for the prestressed membrane supported by discs of small radius. This is a representative example of problems posed over domains with small exclusions, with Neumann conditions applied to the outer boundary and Dirichlet conditions to the boundaries of the exclusions. The first question considered is the choice of underlying mathematical model. In the Basic Model, the discs have finite radii $\sigma_i > 0$. In the Intuitive Model, the physically intuitive limiting case of $\sigma_i = 0$ is taken, which is equivalent to applying point constraints to the membrane. Such “simplifications” occur often enough in engineering practice (see e.g. [4,7,8]), yielding reasonable-appearing FE approximations that can pass common verification tests.

However, point constraints are mathematically inadmissible for such problems, and applying them to the membrane causes the energy of the exact solution to become infinite. Hence this intuitive approach is incorrect. Consequently, the error in the approximations can be unacceptably large. The first source of error is the difference between the exact solution (of the Basic Model) for $\sigma_i > 0$ and its asymptotic limit as $\sigma_i \rightarrow 0$. As shown theoretically in Theorems 5.4 and 5.6 and computationally in Section 7, this can lead to significant differences between the QoI for $\sigma_i > 0$ and their asymptotic limits.

A second source of error arises from trying to approximate an ill-posed problem by the FEM. As shown in Section 8, point constraints are enough to guarantee a unique solution to the FE problem, which moreover are likely to satisfy practically used convergence tests. However, the actual accuracy can be very poor, not only because of the

asymptotic error already mentioned, but also because the FE approximations can be significantly different for different meshes. Consequently, common verification tests for the Intuitive Model cannot be trusted, and results obtained from it must be interpreted with a great deal of caution.

The take-away is that a mathematics-informed approach is needed towards such problems, formulating which is the second issue addressed in this paper. The fundamental ingredient of this approach is to use the Basic Model (7)–(9) for the solution w . The second ingredient is to transform the problem into one whose limit remains bounded in L_2 as $\sigma \rightarrow 0$. This avoids the computationally undesirable effect of the solution getting large everywhere. The reformulated solution (u, A) satisfies (15)–(18), where A is a new unknown representing the vertical distance the holes can move up or down.

The third ingredient is to use *a priori* information of the existence of logarithmic singularities at the holes in designing the FEM. Essentially, these singularities are carried over to the computed solution, and only the smooth remainder is approximated by finite elements. The holes are not meshed, and a uniform grid can be used. This modified FEM is summarized as follows:

Step 1. Define the logarithmic singularities ϕ_i , $i = 1, 2, \dots, n$ by (20).

Step 2. Calculate FE approximations $\psi_{i,h}$ to the components of the smooth remainder, using Eqs. (69)–(70).

Step 3. Use ϕ_i , $\psi_{i,h}$ to form the $(n+1) \times (n+1)$ system of linear equations (74)–(75), and solve it to obtain coefficients $(c_{i,h}, d_h)$.

Step 4. Use ϕ_i , $\psi_{i,h}$, $c_{i,h}$, d_h in the linear combination (80) to get U_h , the approximation to u or W_h , the approximation to w .

Since only smooth functions are approximated, the FEM gives high (optimal) convergence without any special refinement, thus saving the (human) cost involved in meshing the holes. Theorems 6.2 and 6.3 show the uniform h version with degree p essentially yields $O(\kappa^4 + h^{2p})$ convergence in the energy and $O(\kappa^2 + h^p)$ in the force (where the radii are proportional to κ). Computational results presented in Section 7 demonstrate good agreement with these asymptotic estimates for a practical range of parameters.

The modified FE approach can be generalized to anisotropic materials and different operators (such as elasticity or the 3D Laplacian) by adjusting the singularities used in Step 1 (see Remarks 3.2 and 4.3). It can also be generalized to holes of arbitrary shape by changing the coefficients in Eq. (75) used in Step 3 (see Remark 3.1). Higher-order (in κ) extensions can also be formulated (see Remark 5.1). The method is not needed for other pairings of Dirichlet and/or Neumann boundary conditions (see Remark 2.2).

To conclude, the mathematics-informed approach demonstrates the important role that an understanding of the underlying analytic situation plays. In the absence of such understanding, computations obtained using intuitive methods can appear deceptively convincing and lead to erroneous results.

Acknowledgment

We wish to thank Professor Barna Szabó for helpful discussions concerning this work.

References

- [1] M. Ainsworth, J.T. Oden, *A posteriori error estimation in finite element analysis*, in: Pure and Applied Mathematics (New York), Wiley-Interscience [John Wiley & Sons], New York, 2000, p. xx+240.
- [2] I. Babuška, T. Strouboulis, *The finite element method and its reliability*, in: Numerical Mathematics and Scientific Computation, The Clarendon Press, Oxford University Press, New York, 2001, p. xii+802.
- [3] I. Babuška, J.R. Whiteman, T. Strouboulis, *Finite Elements. An Introduction to the Method and Error Estimation*, Oxford University Press, Oxford, 2011, p. xii+323.
- [4] R.P. Feynman, R.B. Leighton, M. Sands, *The Feynman lectures on physics. Vol. 2: Mainly electromagnetism and matter*, Addison-Wesley Publishing Co., Inc., Reading, Mass.-London, 1964, p. xii+569 (not consecutively paged).
- [5] L.N. Trefethen, *Surprises of the Faraday cage*, SIAM News 49 (06) (2016).
- [6] S.J. Chapman, D.P. Hewett, L.N. Trefethen, *Mathematics of the Faraday cage*, SIAM Rev. 57 (3) (2015) 398–417.
- [7] A. Rutman, C. Boshers, L. Pearce, J. Parady, *Fastener modeling for joining composite parts*, in: 2009 Americas Virtual Product Development Conference, M-VPD09-006, 2009.
- [8] B. Szabó, I. Babuška, *Finite Element Analysis*, A Wiley-Interscience Publication, John Wiley & Sons, Inc., New York, 1991, p. xvi+368.
- [9] A.M. Il'in, *Study of the asymptotic behavior of the solution of an elliptic boundary value problem in a domain with a small hole*, Trudy Sem. Petrovsk. (6) (1981) 57–82.
- [10] A.M. Il'in, *Matching of asymptotic expansions of solutions of boundary value problems*, in: Translations of Mathematical Monographs, vol. 102, American Mathematical Society, Providence, RI, 1992, p. x+281. Translated from the Russian by V. Minachin [V.V. Minakhin].

- [11] V. Maz'ya, S. Nazarov, B. Plamenevskij, Asymptotic theory of elliptic boundary value problems in singularly perturbed domains, in: *Operator Theory: Advances and Applications*, vols. I–II, Birkhäuser Verlag, Basel, 2000.
- [12] V. Maz'ya, A. Movchan, M. Nieves, Green's kernels and meso-scale approximations in perforated domains, in: *Lecture Notes in Mathematics*, vol. 2077, Springer, Heidelberg, 2013, p. xviii+258.
- [13] M. Lanza de Cristoforis, Perturbation problems in potential theory, a functional analytic approach, *J. Appl. Funct. Anal.* 2 (3) (2007) 197–222.
- [14] M. Lanza de Cristoforis, Asymptotic behavior of the solutions of the Dirichlet problem for the Laplace operator in a domain with a small hole. A functional analytic approach, *Analysis (Munich)* 28 (1) (2008) 63–93.
- [15] M. Dalla Riva, P. Musolino, Real analytic families of harmonic functions in a planar domain with a small hole, *J. Math. Anal. Appl.* 422 (1) (2015) 37–55.
- [16] M. Dalla Riva, P. Musolino, S.V. Rogosin, Series expansions for the solution of the Dirichlet problem in a planar domain with a small hole, *Asymptot. Anal.* 92 (3–4) (2015) 339–361.
- [17] J. Pommier, B. Samet, The topological asymptotic for the Helmholtz equation with Dirichlet condition on the boundary of an arbitrarily shaped hole, *SIAM J. Control Optim.* 43 (3) (2004) 899–921 (electronic).
- [18] H. Ammari, H. Kang, High-order terms in the asymptotic expansions of the steady-state voltage potentials in the presence of conductivity inhomogeneities of small diameter, *SIAM J. Math. Anal.* 34 (5) (2003) 1152–1166.
- [19] V. Bonnaillie-Noël, M. Dambrine, S. Tordeux, G. Vial, Interactions between moderately close inclusions for the Laplace equation, *Math. Models Methods Appl. Sci.* 19 (10) (2009) 1853–1882.
- [20] E. Bonnetier, D. Manceau, F. Triki, Asymptotic of the velocity of a dilute suspension of droplets with interfacial tension, *Quart. Appl. Math.* 71 (1) (2013) 89–117.
- [21] M.S. Vogelius, D. Volkov, Asymptotic formulas for perturbations in the electromagnetic fields due to the presence of inhomogeneities of small diameter, *M2AN Math. Model. Numer. Anal.* 34 (4) (2000) 723–748.
- [22] G.J. Fix, S. Gulati, G.I. Wakoff, On the use of singular functions with finite element approximations, *J. Comput. Phys.* 13 (1973) 209–228.
- [23] S.E. Benzley, Representation of singularities with isoparametric finite elements, *Internat. J. Numer. Methods Engrg.* 8 (3) (1974) 537–545.
- [24] I. Babuška, G. Caloz, J.E. Osborn, Special finite element methods for a class of second order elliptic problems with rough coefficients, *SIAM J. Numer. Anal.* 31 (4) (1994) 945–981.
- [25] I. Babuška, U. Banerjee, J.E. Osborn, Generalized finite element methods –main ideas, results, and perspectives, *Int. J. Comput. Methods* 1 (2004) 67–103.
- [26] I. Babuška, J.M. Melenk, The partition of unity method, *Internat. J. Numer. Methods Engrg.* 40 (4) (1997) 727–758.
- [27] T.-P. Fries, T. Belytschko, The extended/generalized finite element method: an overview of the method and its applications, *Internat. J. Numer. Methods Engrg.* 84 (3) (2010) 253–304.
- [28] D.L. Clements, Fundamental solutions for second order linear elliptic partial differential equations, *Comput. Mech.* 22 (1) (1998) 26–31.
- [29] T. Strouboulis, L. Zhang, I. Babuška, Generalized finite element method using mesh-based handbooks: application to problems in domains with many voids, *Comput. Methods Appl. Mech. Engrg.* 192 (28–30) (2003) 3109–3161. *Multiscale computational mechanics for materials and structures* (Cachan, 2002).
- [30] S.C. Brenner, L.R. Scott, *The mathematical theory of finite element methods*, third ed., in: *Texts in Applied Mathematics*, vol. 15, Springer, New York, 2008, p. xviii+397.
- [31] I. Babuška, M. Suri, The optimal convergence rate of the p -version of the finite element method, *SIAM J. Numer. Anal.* 24 (4) (1987) 750–776.
- [32] R. Scott, Finite element convergence for singular data, *Numer. Math.* 21 (1973/74) 317–327.